A major purpose of the Technical Information Center is to provide the broadest dissemination possible of information contained in DOE's Research and Development Reports to business, industry, the academic community, and federal, state and local governments.

Although a small portion of this report is not reproducible, it is being made available to expedite the availability of information on the research discussed herein.

LA-UR -85-2964

CONF-8508119--1

Los Alamos National Laboratory is operated by the University of California for the United States Department of Energy under contract W-7405-ENG-36

LA-UR--85-2964

DE85 017543

TITLE COHERENT AND SPONTANEOUS RAMAN SPECTROSCOPY IN SHOCKED AND UNSHOCKED LIQUIDS

AUTHOR(S) S. C. Schmidt, D. S. Moore, D. Schiferl, M. Chatelet, T. P. Turner, J. W. Shaner, D. L. Shampine, W. T. Holt

SUBMITTED TO NATO Advanced Study Institute: Advances in Chemical Reaction Dynamics
Iraklion, Crete, Greece
25 August - 7 September, 1985

DISCLAIMER

Los Alamos National Laboratory
Los Alamos, New Mexico 87545

COHERENT AND SPONTANEOUS RAMAN SPECTROSCOPY IN SHOCKED AND UNSHOCKED LIQUIDS*

S. C. Schmidt, D. S. Moore, D. Schiferl,
M. Chatelet, T. Turner, J. W. Shaner,
D. L. Shampine, and W. T. Holt
University of California
Los Alamos National Laboratory
P. O. Box 1663
Los Alamos, New Mexico 87545, USA

Coherent and non-coherent Raman spectroscopy is being used to study the structure and energy transfer in molecular liquids at high pressures. Stimulated Raman scattering, coherent anti-Stokes Raman scattering, and Raman induced Kerr effect scattering measurements have been performed in liquid benzene and liquid nitromethane shocked to pressures up to 11 GPa. Frequency shifts were observed for the 992 cm^{-1} ring stretching mode of benzene and the 920 cm^{-1} CN stretching mode of nitromethane. Results of these dynamic experiments are compared to spontaneous Raman scattering measurements made in a high temperature diamond anvil cell. Also, a picosecond infrared pump/spontaneous anti-Stokes Raman probe experiment is being used to measure CH stretch vibrational relaxation times in liquid halogenated methanes statically compressed to a few tenths GPa.

*Work supported by the United States Department of Energy.

I. INTRODUCTION AND OBJECTIVES

Presently most models of explosive and shock induced chemical behavior treat the medium as a continuum[1,2] that chemically reacts according to either a pressure dependent or Arrhenius kinetics rate law. One or more parameters are used to incorporate the global chemical behavior, hydrodynamic phenomenology and effects of material heterogeneity. In the past few years, several studies[3-10] have been started that attempt to improve the methodology by defining the continuum, not as a single component, but as one that incorporates ideas such as hot spots, voids or multicomponents. However, in all of these studies essentially no effort is made to incorporate any of the microscopic details of the shock-compression/energy transfer and release phenomenology that constitutes the detonation or reactive process.

Ideally, for descriptions of reactive processes, we would like to treat the continuum as a mixture of pure components and incorporate changes in molecular structure resulting from shock compression, disequlibria due to shock compression, energy transfer from the hydrodynamic mode into the molecular internal degrees of freedom and the subsequent microscopic reaction history, energy release, and product formation. While such a goal may appear overly ambitious we feel that by using some of the diagnostics, particularly fast optical techniques, that have become available in the past few years, progress can be made toward understanding certain facets of this objective. For example, spontaneous Raman spectroscopy has already been used to make temperature estimates of shocked explosives[11-13] and examine the structure of shock-compressed materials.[14-15] In our own work, coherent Raman scattering techniques have been used to measure vibrational frequency shifts in benzene and nitromethane shock-compressed to pressures just below those where chemical reaction is expected.[16-22] Initial indications suggest the prospects for extending these measurements into the pressure regions where chemical reaction occurs are good.

Figure 1 depicts some of the consequences of the shock-compression of molecular materials. In addition to the macroscopic continuum effects expected (e.g. hydrodynamic flow, density and temperature increases), molecular systems, because of vibrational and electronic energy levels that possibly lie close to the ground state, are expected to readily undergo a shock induced transfer of energy to these internal degrees of freedom. Under shock-compression, the molecular structure and hence the intramolecular and intermolecular forces will be altered considerably, consequently the energy transfer rates and mechanisms may be dramatically different from those expected on the basis of either extrapolation from ambient conditions or thermodynamic equilibrium. Depending on the vibrational and electronic relaxation rates and mechanisms in the high density/high temperature fluid, the excited states could have a nonequilibrium population density. Different authors[23-25] have proposed different initial steps for the chemical reaction schemes in detonating explosives. However, definitive supporting experiments have not been performed. The ensuing microscopic chemical reactions involving energy release and product formation also require experimental study.

The objective of our work has been two fold; (1) to determine the molecular structure and identify chemical species in unreacting and reacting shock-compressed molecular systems and (2) to study the effect of pressure and temperature on condensed phase energy transfer. Also, we would like to identify the unique features of a shock wave which contribute to the energy transfer processes. Achievement of these goals would contribute significantly to understanding the initial mechanisms governing shock-induced chemically reacting molecular systems and possibly to the steps controlling product formation. Two experiments are being employed in the pursuit of these objectives. A two-stage light gas gun is being used to dynamically shock-compress molecular liquids to pressures where chemical reaction occurs. The high density/high temperature fluid is then probed using coherent Raman scattering techniques. In the second effort which is still in the construction phase, a picosecond pump/spontaneous anti-Stokes Raman scattering probe experiment will be used to measure vibrational relaxation rates in liquids statically compressed using high pressure cells.

II. EXPERIMENTAL CONSIDERATIONS

Prior to discussing our experimental studies and results to date, several problems associated with conducting condensed-phase shock-vave experiments will be revieved. These difficulties have historically limited the ability to conduct experiments in the adverse conditions through and immediately behind the shock-front and for our studies strongly governed the experimental techniques used.

For many materials shock vaves are believed to be of the order of 1 μm or less in tnickness.[26-28] The passage time through the front of a 1 μm-thick shock whose velocity is 5 km/s is thus of the order of 200 ps or less. Hence, if ve desire to temporally and spatially resolve a measurement through a shock-front (5 data points), the diagnostic technique selected must be capable of spatial and temporal resolutions of 0.2 μm and 40 ps, respectively. Condensed-phase chemical reaction times could be of the order of 1 ps, thus necessitating even better temporal resolution. However, if all that is desired is to resolve features in the few mm long region behind the shock-front where relaxation and reaction processes may occur, then these requirements are drastically reduced.

Optical techniques offer some potential for achieving measurements within these stated limitations. However, with such methods some additional complications arise. Many materials are opaque or become opaque when shock-compressed. Consequently, the use of optical diagnostic techniques is limited to a few select materials primarily for phenomenological studies. Such studies may, however, have tremendous potential when used in conjunction with other techniques for determining phenomenology of shock-compressed materials. Two other difficulties inherent in optical shock-vave diagnostic techniques are the changes in material refractive index that accompany the density changes characteristic of shock waves and the possibility of photochemistry induced by the optical probes. Figure 2 shows the path deviation that occurs when an optical beam is passed through a hypothetical shock-compressed system. The trailing shock vave near the sample boundaries tends to bend the optical beam away from the shock-front thus making prediction of the

expected optical path difficult. Any shock-front curvature will compound this difficulty. If the shock velocity in the windows is greater than in the sample, additional complications could arise from the effect of the more complex wave structure on window transmission. Many molecules undergo photochemical reactions when exposed to light, particularly that in the ultraviolet region of the spectrum. If these reactions are fast compared to the characteristic time of the optical diagnostic, measurements could include the effects of both the shock stimulus and the photochemical reaction.

Measurements made using inhomogeneous samples often are averages over the nonuniformities and consequently do not reflect the details of the microstructure. For materials like granular explosives, the inhomogeneous nature is readily apparent and experiments are interpreted accordingly. For samples thought to be homogeneous, ambiguities can arise. For example, Fig. 3 depicts two image-intensifier-camera pictures[29] of the shock-front of detonating nitromethane and an 80% nitromethane/20% acetone mixture. These pictures show that microstructure exists in the vicinity of the shock front even in liquids, which are often thought to be homogeneous. Also, nothing is known about microstructure in the region immediately behind the shock front. When performing experiments on nitromethane or similar substances, especially experiments utilizing optical techniques where a spatial resolution of tens of microns is desired, one must be aware that results may actually reflect an average over a smaller characteristic microstructure. Conversely, a single measurement with spatial resolution smaller than the microstructure may be misinterpreted as representative of the average material.

Shock recovery experiments are often used to observe chemical and physical changes through and immediately behind the shock-front. However, these changes occur not only in the high pressure and temperature region at the shock front, but also in the somewhat lower pressures and temperatures of the expansion region. The inability to separate these two effects makes the interpretation of these experiments difficult.

III. COHERENT RAMAN SCATTERING IN SHOCK-COMPRESSED LIQUIDS

Three coherent Raman scattering techniques have been attempted in shock compressed liquid samples. Advantages of these techniques, primarily because of large scattering intensities and the beam-like nature of the scattered signal, are increased detection sensitivity, temporal resolution limits approaching laser pulse lengths, and possible spatial resolution approaching the diffraction limit of the optical components. As with all optical methods in shock-wave applications, optical accessibility because of material opacity or particulate scattering remains a major difficulty with coherent Raman scattering.

Backward-stimulated Raman scattering (BSRS) has been observed in shock-compressed benzene up to pressures of 1.2 GPa.[17] Stimulated Raman scattering[30,31] (Fig. 4) occurs when the incident laser intensity in a medium exceeds a threshold level and generates a strong, stimulated Stokes beam. The threshold level is determined by the Raman cross-section and linewidth of the transition and by the focusing parameters of the incident beam. Typical threshold intensities are ~ 10-100 GW/cm^2. Figure 5 illustrates the arrangement used for the backward stimulated Raman scattering experiment. An aluminum projectile of known velocity from a 51-mm-diam, 3.3-m-long gas gun impacted an aluminum target plate producing a shock wave which ran forward into a 7.5 to 8-mm-thick reagent grade benzene sample (Mallickrodt, Inc.). Standard data reduction techniques[32] using published shock-velocity/particle-velocity data[33] were used to determine the state of the shock-compressed benzene. Experiment design was greatly facilitated using the MACRAME one-dimensional-wave propagation computer code.[34]

A single 6-ns-long frequency-doubled Nd-doped yttrium aluminum garnet (Nd:YAG) laser pulse was focused using a 150-mm focal length lens through the quartz window to a point in the benzene 2 to 6 mm in front of the rear sample wall. The high intensity of the laser at the focus, coupled with the presence of a large cross-section Raman active vibrational mode in the sample, produces gain in the forward and backward directions along the beam at a frequency that is different from the

Nd:YAG frequency by the frequency of the active mode. The timing sequence was determined by the incoming projectile. Interruption of a HeNe laser beam, in conjunction with an appropriate time delay, triggered the laser flash lamp approximately 300 μs prior to impact. A time-of-arrival pin activated just before impact and the appropriate time delay served to Q-switch the laser just prior to the shock wave striking the quartz window and after it was past the focal point of the incident laser light.

In liquid benzene, the ν_1 symmetric stretching mode[35] at 992 cm^{-1} has the lowest threshold for stimulated Raman scattering induced by 532-nm light, and was the transition observed in these experiments. As depicted in Fig. 5, the backward stimulated Raman beam was separated from the incident laser by means of a dichroic filter and was then focused onto the 10-μm-wide entrance slit of a 1-m Czerny-Turner spectrograph equipped with a 1200-grooves/nm grating blazed at 500 nm and used in first order. Figure 6 shows the resulting spectrogram for benzene shock-compressed to 0.92 GPa. The reflected incident laser line and the backward stimulated Brillouin-scattering line at 532 nm are observable, as are the backward stimulated Raman-scattering line from ambient benzene. The latter feature resulted as a consequence of the shock wave having passed only about two-thirds of the way through the sample, and hence a stimulated Raman signal was also obtained from the unshocked liquid.

The frequency shift of the Raman line has small contributions of approximately 0.1 cm^{-1} because the light crosses the moving interface between two media of different refractive indices and because of the material motion behind the shock wave.[36] Since these errors are considerably less than the experimental uncertainty of $\pm$ 0.5 cm^{-1} for the measured frequency shifts and are a small fraction of the shift due to compression, no attempt was made to correct the data for these effects.

Figure 7 gives the measured shift of the ν_1 ring-stretching mode vibrational wavenumber versus pressure of the shocked benzene. Observation of the ring-stretching mode at 1.2 GPa strongly suggests that

benzene molecules still exist several millimeters behind the shock wave at this pressure, but does not, however, exclude some decomposition.[27,37,38]

Also depicted in Fig. 7 is the ring-stretching mode vibrational wavenumber shift measured for benzene isothermally compressed at temperatures between 24°C and 209°C with a diamond-anvil cell and techniques previously described.[39] Measurements of the phonon spectrum in the region 40-200 cm^{-1} were used to distinguish between benzene I, benzene II, and liquid benzene. The vibrational frequencies obtained from spontaneous-Raman-scattering measurements at 24°C with use of the 568.2-nm line of a krypton laser agree well with previous results for benzene.[35]

At fixed pressure, no temperature shift was observed in these static measurements. The wavenumber shifts for the dynamic experiments agree well with the static data for either liquid benzene or benzene II, but differ substantially from those for benzene I. At pressures below the I-II-liquid triple point near 1.2 GPa,[40,41] the shocked benzene is therefore probably at temperatures high enough for it to be in the liquid state. At pressures near 1.2 GPa, the shock-compressed material could be either liquid or benzene II since both phases exhibit about the same magnitude of wavenumber shift for the ring-stretching mode, and the Hugoniot lies close to the phase boundary.

Beam intensities using BSRS are sufficiently large that film can be used as a detector. The large incident intensities required, however, can cause damage to optical components near focal points. Spatial and temporal resolution are determined by the confocal parameter of the focusing lens and the incident laser pulse duration. The BSRS technique also suffers because only certain molecules produce stimulated Raman scattering and of those molecules only the lowest threshold transition can be observed. Because of these limitations other coherent Raman scattering processes affording more experimental flexibility were attempted.

Coherent anti-Stokes Raman scattering (CARS)[42-45] (Fig. 4) occurs as four-wave parametric process in which three waves, two at a pump frequency, ω_p, and one at a Stokes frequency, ω_s, are mixed in a sample to produce a coherent beam at the anti-Stokes frequency, $\omega_{as} = 2\omega_p - \omega_s$. The efficiency of this mixing is greatly enhanced if the frequency difference $\omega_p - \omega_s$ coincides with the frequency of a Raman active mode of the sample. An advantage of CARS is that it can be generated at incident power levels considerably below those required for stimulated Raman scattering. However, since phase matching is required, possible geometrical arrangements are limited.

A schematic of the experimental apparatus used to perform reflected broadband coherent anti-Stokes Raman scattering (RBBCARS) in shock-compressed benzene and nitromethane is shown in Fig. 8. For pressures greater than 2 GPa, a two-stage light-gas gun was used to accelerate a polycarbonate projectile with 4-mm-thick AZ31B magnesium or 2024 aluminum impactors to a desired velocity. The projectile struck an approximately 2.4-mm-thick 304-stainless-steel target plate producing a shock wave which ran forward into a 2.7-mm to 3.3-mm-thick benzene (or nitromethane) sample. Lower pressures were achieved using the previously described technique for backward stimulated Raman scattering. Stainless steel was chosen as the target plate because of previous experience and a series of reflectivity measurements which showed that polished steel would retain approximately 20 percent of its original reflectivity under shock compression at 11 GPa in the liquid sample (approximately 70 GPa in the stainless steel). This was necessary to reflect the CARS signal back out of the shock-compressed liquid. Reagent grade benzene (Mallinckrodt, Inc.) and commercial grade (Angus Chemical Co.) nitromethane were used. The state of the shock compressed material was determined as described above.

The timing sequence for the RBBCARS experiment was determined by the incoming projectile. A signal from three HeNe laser/photodiode detectors located in the barrel approximately 2.8, 1.2 and 0.7 m from the target, in conjunction with an appropriate time delay, triggered the laser flash lamps approximately 300 μs prior to impact. A time-of-arrival pin acti-

vated just after the shock entered the liquid and another time delay served to Q-switch the laser approximately when the shock vave arrived at the quartz vindov.

Since the Raman frequencies of the shock-compressed materials are not precisely known, and since ve vish to produce CARS signals from more than one mode or species, a broadband dye laser, vith a bandvidth equivalent to the gain profile of the dye, vas used as the Stokes beam.[46] A portion of the 6-ns-long frequency-doubled Nd:YAG laser pulse vas used to pump the dye laser. The dye laser beam was passed through a Galilean telescope and sent along a path parallel to the remaining pump laser towards the sample. The beams were focused and crossed (with approximately 1-mm length of overlap) at a point approximately 1 mm in front of the vindov using a previously described technique.[47] The beam crossing angle (phase-matching angle) vas tuned by adjusting the distance between the parallel beams using a turning mirror on the pump laser beam. The CARS beam was reflected out of the shocked sample by the highly polished front surface of the target plate and along a path parallel to the two incoming beams. After being separated from the pump and Stokes beams using a long-wavelength-pass dichroic filter, the beam vas focused onto the 100 μm-wide entrance slit of a 1-m spectrometer equipped with a 1200 l/mm grating blazed at 500 nm and used in first order. The signals vere detected at the exit of the spectrometer using an intensified diode array (Tracor Northern Model TN-6133) coupled to an optical multichannel analyzer (OMA) (Tracor Northern Model TN-1710). The instrument spectral resolution vas approximately 4.2 cm^{-1}.

Figure 9 shovs the OMA recorded RBBCARS signals for the ring-stretching mode of benzene at pressures from ambient to 10.6 GPa (approximately 1000 ^{o}K).[48] Spectral positions were measured relative to the 253.652-nm Hg emission line in second order.

A preliminary analysis of the spectral lines vas performed using:[44]

$$I_{as} \propto \omega_{as}^2 |\chi^{(3)}|^2 I_s \qquad (1)$$

where I_{as} and I_s are the intensities of the anti-Stokes and Stokes beams respectively. For this calculation, I_s was chosen to be a Gaussian that approximately fit the broad band dye laser profile. In future experiments, because of shot-to-shot variations and noise in the dye laser profile, a spectrographic record will be made of the profile for each shot and used directly to calculate the synthetic spectra. The third order susceptibility, $\chi^{(3)}$, is given by

$$\chi^{(3)} = \chi_{NR} + \sum_j \chi_j' + i \sum_j \chi_j'' \tag{2}$$

where χ_{NR} is the contribution from the nonresonant background and j is the sum over spectral lines. The real, χ_j', and imaginary, χ_j'', parts of the CARS susceptibility are

$$\chi_j' = \frac{\Gamma_j \chi_j (\omega_j - \omega_p + \omega_s)}{(\omega_j - \omega_p + \omega_s)^2 + \Gamma_j^2} \tag{3}$$

and

$$\chi_j'' = \frac{\Gamma_j^2 \chi_j}{(\omega_j - \omega_p + \omega_s)^2 + \Gamma_j^2} \tag{4}$$

respectively. ω_j, Γ_j and χ_j are the frequency, half amplitude half width (HWHM) and the peak amplitude of the corresponding spontaneous Raman scattered line. For this work no attempt was made to derive population densities (or temperatures) from χ_j using known Raman cross-sections. In fact, it may be necessary to re-determine the Raman cross-sections for the high densities characteristic of shock-compression.

Figure 10 depicts the experimentally measured and calculated spectra for the benzene ring stretching mode at 7.4 GPa. The intensity of both spectra has been normalized to a peak amplitude of 0.95. The structural

features that appear in the measured spectra are thought to result from the noise in the broad band dye laser. An initial analysis of the spectral shape at 10.6 GPa is dramatically different and requires two spectral lines to fit the measured profile. This will be discussed in a future publication.

The frequency shifts estimated for the 7.4 GPa line and the lines at other pressures are depicted in Fig. 7 along with the frequency shifts determined from BSRS measurements discussed previously. The results show an initial linear change of the frequency shift with pressure and then a weakening of this dependence as the region near 13 GPa is approached. Previous work[27,37,38,49,50] suggests chemical reaction occurs at these pressures. A plot of frequency shift versus volume change shows a non-linear dependence at all pressures.

The RBBCARS spectra for the CN stretching mode of nitromethane at pressures from ambient to 7.6 GPa (approximately 950 ^{o}K)[51] are shown in Fig. 11. The existence of the CN mode at microsecond times after shocking implies that decomposition of the nitromethane has not occurred as has been observed for times of tens of microseconds[52] and in static high temperature/high pressure studies.[53] Measurements are presently being extended to higher pressures where nitromethane is thought to be reactive for very short shock run distances.[12,48,54-56]

Synthetic spectra were obtained for the nitromethane CN stretch mode using the procedure previously described for benzene. Figure 12 shows the experimentally measured and calculated spectra for 5.5 GPa normalized to a peak intensity of 0.95. At 5.5 GPa and for the lower pressure nitromethane spectra, this preliminary analysis suggests that the spectral signatures are much better matched using two spectral lines separated by approximately 10 cm^{-1}. This second line has been observed previously in static high pressure Raman spectra.[57] The fitting at 7.6 GPa required a minimum of four or five spectral lines to represent the measured data. Discussion of these results will be withheld for a future publication when more accurate synthetic spectra can be calculated using measured dye laser profiles.

Figure 13 shows the estimates for the Raman frequency shifts of the more intense spectral feature versus pressure using the analysis indicated above. Also depicted are the frequency shifts measured for the CN stretch mode of solid nitromethane using a diamond anvil high pressure cell[58] and the spontaneous Raman measurements for nitromethane shocked to pressures of 5 GPa.[12] It is noted that our results obtained for the shock-compressed material do not differ significantly from the Raman shifts obtained for solid nitromethane. At present, we do not have an explanation for the difference between our results and those obtained by Delpeuch and Menil[12] using spontaneous Raman scattering. Earlier results[11] by these authors agreed more closely with our results. The plot of frequency shift versus volume change was very similar to that observed for benzene.

Raman-induced Kerr effect spectroscopy (RIKES)[59] has been discussed as a diagnostic technique[19,20,60] for performing measurements in shock-compressed systems which may have a large non-resonant background. RIKES requires a single frequency pump beam, a broad-band probe source, no phase matching and lower incident power levels than stimulated Raman scattering (Fig. 4).

The effect can be described in terms similar to the above description of CARS. A linearly polarized probe laser beam is passed through the rotating electric field of a circularly polarized pump beam. The four-wave parametric process described above induces an ellipticity on the probe beam whenever the frequency difference between the two lasers equals that of a Raman active transition in the sample.[61,62] Since the RIKES involves the use of a single frequency pump laser and a broadband Stokes laser, it can be performed with an apparatus very similar to the above described RBBCARS apparatus. The modifications necessary are shown in Fig. 14 and are described below. The portion of the frequency-doubled Nd:YAG laser beam that does not pump the dye laser is passed through a Fresnel rhomb to produce a beam of > 99% circular polarization. The dye laser beam (Stokes frequencies) is passed through a high quality Glan-Taylor (air-gap) prism to produce a beam of ~ 1 part in 10^6 linear polarization. The two beams are focused and crossed in the sample using

a 150 mm focal length, 50 mm diameter lens. The crossing angle is near 6 degrees, giving an overlap length of ~ 150 μm at the focus. The Stokes beam is then reflected by the highly polished front surface of the target plate back through the sample and along a path parallel to the incoming beams. A mirror separates the reflected dye laser beam from the other beams and directs it first through a Babinet-Soliel polarization compensator and then through a Glan-Taylor polarization analyzer. The compensator was found to be necessary to remove the ellipticity introduced into the linearly polarized Stokes laser beam by the birefringence inherent in the optical components located between the polarizers, including the ambient sample. When the two Glan-Taylor prisms are crossed, the dye laser beam is blocked except at frequencies corresponding to Raman resonances, where the RIKES signals are passed. These signals are directed through a dove prism, focused into the entrance slits of the 1 m spectrometer and detected by the OMA system.

Figure 15 shows two RIKES 992 cm^{-1} region spectra of benzene shock-compressed to 1.17 GPa. Both traces have spectral features, however they are not consistent and do not exhibit the pressure-induced frequency shift expected for the benzene ring stretching mode based on previous BSRS and RBBCARS experiments. In a polarization sensitive coherent Raman experiment, such as RIKES, the possibility exists that shock-induced changes in a material would perturb the probe laser polarization sufficiently to obscure the desired signals. Therefore, the sensitivity of the RIKES apparatus to minor rotations of the dye laser polarization was investigated. The figure of merit used was the polarization analyzer rotation angle necessary to saturate the detector with unblocked dye laser. It was found that the detector could be driven from zero signal to saturation with a polarization rotation angle of ~ 20 arc minutes (20′) (using 50 μm slits and 50 μJ dye laser energy). The RIKES signal found for the ring-stretching mode of ambient liquid benzene nearly saturated the detector through 25 μm slits (using ~ 200 μJ pump laser energy and 6° beam crossing angle). These data suggest that, if the shock-compressed sample induced a rotation of the probe laser polarization $\gtrsim$ 20′, the signal would be masked by the broad dye laser background passed by the analyzer. The RIKES spectra (Fig. 15) obtained in shocked

samples show only broadband dye laser which has been passed by the polarization analyzer. These results indicate that the shock-compressed sample induces a rotation of at least 20° on the dye laser polarization. They also lead to the conclusion that, while it may be possible to perform RIKES experiments in shock-compressed materials in spite of our failure, the experiment is considerably more difficult than techniques not sensitive to the absolute polarization of the laser beam (such as BSRS and RBBCARS).

IV. ENERGY TRANSFER IN HIGH PRESSURE LIQUIDS

Although an abundance of literature[63-80] exists describing condensed phase energy transfer and relaxation phenomenology at ambient pressures and various temperatures, there is a dearth of studies showing behavior as a result of high pressure,[81-83] of large stress gradients, and of temperatures typical in shock-wave environments. Since understanding condensed phase molecular energy transfer is fundamental to understanding shock-induced chemical reactions and detonation, we have initiated an experiment to study the effects of pressure and temperature on condensed phase energy transfer. The experiment is based on the picosecond relaxation experiments of Laubereau et al.[84,85] and Fendt et al.[86] and ultrasonic studies of Takagi et al.[74,75] which study the vibrational energy transfer in substituted methanes. These materials were chosen because they have a simple molecular structure and have relaxation times comparable to those expected in shock compressed hydrocarbons. The lower vibrational energy levels and some overtone and combination levels in the vicinity of the CH stretch levels near 3000 cm^{-1} are shown in Fig. 16 for dichloromethane, dibromomethane and diiodomethane. The results of the studies for dichloromethane show that after populating the CH stretch modes using a picosecond infrared laser pulse (equilibration between the two modes is very rapid) these levels decay through a weak Fermi resonance to an overtone level of the bending modes. The presence of the Fermi resonance is deduced from a line in the infrared spectrum at 2832 cm^{-1} due to the first overtone of the ν_2 bending mode (Fig. 16). ν_1 and ν_6 are the two CH stretching modes and the peak at 2832 cm^{-1} is from $2\nu_2$. We believe that an important aspect of energy transfer during shock

compression and shock-compression chemistry is how the energy flows through the vibrational degrees of freedom, i.e., how they are populated from the translational energy of the shock wave and if they are in equilibrium. In the case of the above system, compression either using shock-wave techniques or statically using a diamond-anvil cell, will induce a relative shift in the ν_1, ν_6 and ν_2 levels that should change the resonant coupling of the CH fundamental levels and the ν_2 overtone. The relaxation time should change accordingly.

Figure 17 schematic shows an experiment to measure the change in the CH stretch mode energy relaxation time at high pressure and temperature. Sub-picosecond pulses from a colliding-pulse-mode-locked ring dye laser[87] will be amplified using an excimer laser driven four stage amplifier and then used to generate picosecond infrared pulses which will vibrationally excite, by infrared absorption, the CH stretch levels of the substituted methanes. Part of the original amplified pulse will be optically delayed and used to probe the population density of the excited state by spontaneous anti-Stokes Raman scattering. Experiment repetition rate is 100 Hz.

The Raman scattering signals will be detected by either a high quantum efficiency photo multiplier tube equipped with suitable filters or in a spectrograph using an optical multichannel analyzer. Compression of the sample to several GPa will be accomplished using a diamond anvil or other high pressure cell.

Experiment details and results will be described in a future publication. It is hoped that this experiment can be used to study the intra- or inter-molecular relaxation phenomenology at densities similar to those existing during shock compression. At pressures of several GPa, the molecules may not exist individually but as some other type of structure with radically shifted energy levels. Interpretation would require a theoretical approach which differs significantly from the frequently used bimolecular collision model.

V. SUMMARY

Fundamental understanding of the detailed microscopic phenomenology of shock-induced chemical reaction and detonation waves is being sought by using pulsed coherent optical scattering experiments to determine the molecular structure, constituents and energy transfer mechanisms in both shock-compressed and static, high pressure/high temperature fluids. To date measurements of the ring stretching mode of benzene and the CN stretching mode of nitromethane up to shock-induced pressures just below those for which reaction is suspected to occur have shown both a shift in the vibrational frequencies and a definite change in the spectral profile. These results have confirmed that these molecules still exist on the microsecond time scale behind the shock front, but that some form of energy transfer is occurring from the hydrodynamic mode to the molecular internal degrees of freedom. Future experiments, both static high pressure picosecond vibrational relaxation and dynamic coherent Raman scattering at shock-compression pressures in the region where reaction is expected, should yield significant insight toward understanding the very complex and rapid processes that prevail in the shock environment.

VI. ACKNOWLEDGEMENTS

The authors wish to thank C. W. Caldwell, R. L. Eavenson, and R. S. Medina for their assistance in performing the shock-compression experiments and V. A. Gurule, C. N. Gomez, and R. W. Livingston for machining and fabrication of the target assemblies. Special thanks is given to J. N. Fritz for use of the MACRAME computer code used to design target assemblies.

VII. REFERENCES

1. C. A. Forest, "Burning and Detonation," LA-7245 (Los Alamos National Laboratory Report, Los Alamos, New Mexico 1978).

2. C. L. Mader, Numerical Modeling of Detonation (University of California Press, Berkeley, California 1979).

3. E. L. Lee and C. M. Tarver, Phys. Fluids 23, 2362 (1980).

4. J. Wackerle, R. L. Rabie, M. J. Ginsberg and A. B. Anderson in Proceedings of the Symposium on High Dynamic Pressures (Commissariat á l'Energie Atomique, Paris, France 1978) p. 127.

5. M. Cowperthvaite in Proceedings of the Symposium on High Dynamic Pressures (Commissariat á l'Energie Atomique, Paris, France 1978) p. 201.

6. J. W. Nunizato in Shock Waves in Condensed Matter - 1983, J. R. Asay, R. A. Graham, and G. K. Straub, eds. (Elsevier Science Publishers B. V., 1984) p. 293.

7. J. W. Nunizato and E. K. Walsh, Arch. Rational Mech. Anal. 73, 285 (1980).

8. J. N. Johnson, P. K. Tang and C. A. Forest, J. Appl. Phys. 57, 4323 (1985).

9. P. K. Tang, J. N. Johnson and C. A. Forest in Proc. 8th Symp. Detonation (Albuquerque, New Mexico 1985), p. 375.

10. C. Mader and J. Kerschner in Proc. 8th Symp. Detonation (Albuquerque, New Mexico 1985) p. 366.

11. F. Boisard, C. Tombini and A. Menil in Proc. 7th Symp. Detonation, (Annapolis, Maryland 1981) p. 531.

12. A. Delpuech and A. Menil, in Shock Waves in Condensed Matter - 1983, J. R. Asay, R. A. Graham, and G. K. Straub, eds. (Elsevier Science Publishers B. V., 1984) p. 309.

13. S. Dufort and A. Delpuech in Proc. 8th Symp. Detonation, Albuquerque, Nev Mexico 1985) p. 221.

14. N. C. Holmes, A. C. Mitchell, W. J. Nellis, W. B. Graham and G. E. Walrafen, in Shock Waves in Condensed Matter - 1983, J. R. Asay, R. A. Graham and G. K. Straub, eds. (Elsevier Science Publisher B.V., 1984) p. 307.

15. W. M. Trott and A. M. Renlund in Proc. 8th Symp. Detonation, (Albuquerque, New Mexico 1985) p. 416.

16. D. S. Moore, S. C. Schmidt, D. Schiferl, and J. W. Shaner, in Los Alamos Conference on Optics '83, R. S. McDowell and S. C. Stotlar, eds. (Proceedings SPIE Volume 380, 1983) p. 208.

17. S. C. Schmidt, D. S. Moore, D. Schiferl, and J. W. Shaner, Phys. Rev. Lett. 50, 661 (1983).

18. D. S. Moore, S. C. Schmidt, and J. W. Shaner, Phys. Rev. Lett. 50, 1819, (1983).

19. S. C. Schmidt, D. S. Moore, and J. W. Shaner, in Shock Waves in Condensed Matter - 1983, J. R. Asay, R. A. Graham, and G. K. Straub, eds. (Elsevier Science Publishers B. V., 1984) p. 293.

20. D. S. Moore, S. C. Schmidt, D. Schiferl, and J. W. Shaner, in High Pressure in Science and Technology, Part II, C. Homan, R. K. MacCrone, and E. Whalley, eds. (North Holland Publishing, New York, 1984) p. 87.

21. S. C. Schmidt, D. S. Moore, J. W. Shaner, D. L. Shampine, and W. T. Holt in Xth AIRAPT High Pressure Conference, University of Amsterdam, Amsterdam, The Netherlands, 8-11 July 1985.

22. D. S. Moore, S. C. Schmidt, J. W. Shaner, D. L. Shampine, and W. T. Holt in Fourth APS Topical Conference on Shock Waves in Condensed Matter, Spokane, Washington, USA, 22-25 July, 1985.

23. A. Delpuech, J. Cherville, and C. Michaud in Proc. 7th Symp. Detonation, (Annapolis, Maryland 1981) p. 36.

24. J. Alster, N. Slagg, M. J. S. Dewar, J. P. Ritchie, and C. Wells in Fast-Reactions in Energetic Systems, C. Capellas and R. F. Walker, eds. (D. Reidel Publishing Co., 1981) p. 695.

25. R. Engelke, W. L. Earl and C. M. Rohlfing, J. of Chem. Phys., to be published.

26. S. B. Kormer, Sov. Phys.-Uspekhi 11, 229 (1968).

27. A. N. Dremin and V. Yu. Klimenko, "On the Role of the Shock Wave Front in Organic Substances Decomposition," Gas Dynamics of Explosions and Reactive Systems, Minsk, USSR 1981.

28. A. N. Dremin, V. Yu. Klimenko, K. M. Michaijuk and V. S. Trofimov in Proc. 7th Symp. Detonation (Annapolis, Maryland 1981) p. 789.

29. W. C. Davis in Proc. 7th Symp. Detonation (Annapolis, Maryland 1981) p. 531.

30. M. Maier, W. Kaiser and J. A. Giordmaine, Phys. Rev. 177, 580 (1969).

31. D. V. J. Linde, M. Maier and W. Kaiser, Phys. Rev. 178, 178 (1969).

32. M. H. Rice, R. G. McQueen and J. M. Walsh, Solid State Physics 6 (Academic Press, New York 1958) p. 1.

33. R. D. Dick, J. Chem. Phys. 57, 6021 (1970).

34. J. N. Fritz, in preparation for publication.

35. W. D. Ellenson and M. Nicol, J. Chem. Phys. 61, 1380 (1974), this mode is called ν_2 in G. Herzberg, Infrared and Raman Spectra (Van Nostrand Reinhold, New York 1968).

36. R. N. Keeler, G. H. Bloom and A. C. Mitchell, Phys. Rev. Lett. 17, 852 (1966).

37. A. N. Dremin and L. V. Barbare in Shock Waves in Condensed Matter - 1981, Am. Inst. Phys. Proc. 78. W. S. Nellis, L. Seaman, and R. A. Graham eds. (New York 1983), p. 270.

38. L. V. Barbare, A. N. Dremin, S. V. Pershin and V. V. Yakovlev, Fiz. Gor. i Var 5, No. 4, 528 (1969).

39. R. LeSar, S. A. Ekberg, L. H. Jones, R. L. Mills, L. A. Schwalbe, and D. Schiferl, Solid State Comm. 32, 131 (1979).

40. S. Block, C. E. Weir, and G. J. Piermarini, Science 169, 586 (1970).

41. J. Akella and G. C. Kennedy, J. Chem. Phys. 55, 793 (1971).

42. P. D. Maker and R. W. Terhune, Phys. Rev. 137, A801 (1965).

43. W. M. Tolles, J. W. Nibler, J. R. McDonald and A. B. Harvey, Appl. Spectrosc. 31, 253 (1977).

44. J. W. Nibler and G. V. Knighten, in Raman Spectroscopy of Gases and Liquids, A. Weber, ed. (Springer-Verlag, Berlin Heidelberg, 1979) p. 253.

45. A. C. Eckbreth and P. W. Schreiber, in Chemical Applications of Nonlinear Raman Spectroscopy, A. B. Harvey, ed. (Academic, New York, 1981), p. 27.

46. W. B. Roh, P. W. Schreiber, and J. P. E. Taran, Appl. Phys. Lett. 29, 174 (1976).

47. J. J. Valentini, D. S. Moore, and D. S. Bomse, Chem. Phys. Lett. 83, 217 (1981).

48. W. J. Nellis, F. H. Ree, R. J. Trainor, A. C. Mitchell and M. B. Boslough, J. Chem. Phys. 80, 2784 (1984).

49. O. B. Yakusheva, V. V. Yakushev and A. N. Dremin, High Temp.-High Pres. 3, 261 (1971).

50. B. W. Dodson and R. A. Graham in Shock Waves in Condensed Matter - 1981, Am. Inst. Phys. Proc. 78, W. S. Nellis, L. Seaman, and R. A. Graham, eds. (New York 1981).

51. P. C. Lysne and D. R. Hardesty, J. Chem. Phys. 59, 6512 (1973).

52. F. E. Walker and R. J. Wasley, Comb. Flame 15, 233 (1970).

53. J. W. Brasch, J. Phys. Chem., 84, 2085 (1980).

54. D. R. Hardesty, Comb. Flame 27, 229 (1976).

55. A. A. Vorob'ev and V. S. Trofimov, Fiz. Gor. i Vzr 18, Nov. 6, 74 (1982).

56. A. N. Dremin, V. Yu. Klimenko and I. Yu. Kosireva in Proc. 3th Symp. Detonation (Albuquerque, New Mexico 1985) p. 407.

57. D. Schiferl, private communication.

58. D. T. Cromer, R. R. Ryan and D. Schiferl, J. Phys. Chem. 89, 2315 (1985).

59. D. Heiman, R. W. Hellworth, M. D. Levenson and G. Martin, Phys. Rev. Lett. 36, 189 (1976).

60. W. G. VonHolle and R. A. McWilliams in Laser Probes for Combustion Chemistry (American Chemical Society Symposium Series 134), D. R. Crosley, ed. (American Chemical Society, Washington, D.C. 1983), p. 319.

61. G. L. Eesley, Coherent Raman Spectroscopy (Pergamon Press, Oxford 1981).

62. M. D. Levenson in: Chemical Applications of Nonlinear Raman Spectroscopy, A. B. Harvey, ed. (Academic Press, New York 1981) pp. 214-222.

63. W. F. Calaway and G. E. Ewing, Chem. Phys. Lett. 30, 485 (1975).

64. W. F. Calaway and G. E. Ewing, J. Chem. Phys. 63, 2842 (1975).

65. C. Manzanares and G. E. Ewing, J. Chem. Phys. 69, 1418 (1978).

66. C. Manzanares and G. E. Ewing, J. Chem. Phys. 69, 2803 (1978).

67. D. W. Chandler and G. E. Ewing, J. Chem. Phys. 73, 4904 (1980).

68. D. W. Chandler and G. E. Ewing, J. Phys. Chem. 85, 1994 (1981).

69. W. Kaiser and A. Laubereau in Nonlinear Spectroscopy (Proc. International School of Physics "Enrico Fermi," Course LXIV), N. Bloemberger, ed. (North-Holland Publishing Co., Amsterdam 1977), p. 404.

70. A. Laubereau and W. Kaiser, Rev. Mod. Phys. 50, 607 (1978).

71. D. Samios and Th. Dorfmuller, Mol. Phys. 41, 637 (1980).

72. Th. Dorfmuller and D. Samios, Mol. Phys. 43, 23 (1981).

73. K. Takagi, P.-K. Choi and K. Negishi, J. Acoust. Soc. Am. 62, 354 (1977).

74. K. Takagi and K. Negishi, J. Chem. Phys. 72, 1809 (1980).

75. K. Takagi, P.-K. Choi and K. Negishi, J. Chem. Phys. 74, 1424 (1981).

76. P.-K. Choi, K. Takagi and K. Negishi, J. Chem. Phys. 74, 1438 (1981).

77. J. T. Yardley, Introduction to Molecular Energy Transfer, (Academic Press, New York 1980).

78. C. Capellos and R. F. Walker, Fast Reactions in Energetic Systems, (D. Reidel Publishing Co., Dordrecht, Holland 1980).

79. P. M. Rentzepis, Science 218, 1183 (1982).

80. J. Chesnoy and G. M. Gale, "Vibrational Energy Relaxation in Liquids," in preparation.

81. M. Chatelet, G. Widenlocher and B. Oksengorn in High Pressure - Science and Technology, Vol. 2, B. Vodar and Ph. Marteau, eds. (Pergamon Press, Oxford 1979), p. 628.

82. M. Chatelet, B. Oksengorn, G. Widenlocher and Ph. Marteau, J. Chem. Phys. 75, 2374 (1981),

83. M. Chatelet, J. Kieffer and B. Oksengorn, to be published Chem. Phys.

84. A. Laubereau, S. F. Fisher, K. Spanner, and W. Kaiser, Chem. Phys. 31, 335 (1978).

85. H. Graener and A. Laubereau, Appl. Phys. B29, 213 (1982).

86. A. Fendt, S. F. Fischer, and W. Kaiser, Chem. Phys. 57, 55 (1981).

87. R. L. Fork, B. I. Greene, and C. V. Shank, Appl. Phys. Lett. 38, 671 (1981).

FIGURE CAPTIONS

Fig. 1. Condensed-phase molecular energy transfer.

Fig. 2. Refractive effects of shock wave on optical beam.

Fig. 3. Detonation wave microstructure for nitromethane and a nitromethane/acetone mixture.[28]

Fig. 4. Coherent Raman scattering techniques.

Fig. 5. Schematic representation of backward stimulated Raman-scattering experiment. SHG, second harmonic generator; Harm. Sep., harmonic separator. Sample, liquid benzene.

Fig. 6. Scattered light spectrogram for shock-compressed benzene.

Fig. 7. Benzene ring-stretching mode vibrational frequency shifts (with respect to 992 cm^{-1}) vs pressure. The solid circles represent data obtained up to pressures of 1.2 GPa using the single stage gas gun and the open circles represent data obtained using the two stage light gas gun. The straight line is a fit of the shock-compressed data at pressures less than 1.2 GPa. The phase of the benzene during the diamond-anvil cell compression has been determined from phonon spectrum measurements. At 24 C benzene I was observed as a metastable phase above 1.2 GPa and benzene II was observed as a metastable phase below this pressure. Both spectrometers were calibrated with liquid benzene at room temperature.

Fig. 8. Schematic representation of the reflected broadband coherent anti-Stokes Raman scattering experiment. SHG - second harmonic generator; Harm. Sep. - harmonic separator; OMA - optical multichannel analyzer; Sample - benzene and nitromethane.

Fig. 9. RBBCARS spectra of ambient and shock-compressed benzene. The ambient peak position of the benzene is 992 cm^{-1}. Shock pressures are indicated. Wavelength calibration was done relative to the 253.652 nm Hg line in second order.

Fig. 10. Spectral fit of 7.4 GPa ring stretching mode of benzene. Wavelength calibration is with respect to the 253.652 nm Hg line in second order and the spectral slit width is 4.2 cm^{-1}.

Fig. 11. RBBCARS spectra of ambient and shock-compressed nitromethane. The ambient peak position is 920 cm^{-1}. Shock pressures are indicated. Wavelength calibration was done with respect to the 253.652 nm Hg line in second order.

Fig. 12. Spectral fit of 5.5 GPa CN stretching mode of nitromethane. Wavelength calibration is with respect to the 253.652 nm Hg line in second order and the spectral slit width is 4.2 cm^{-1}.

Fig. 13. Nitromethane CN stretching mode vibrational frequency shifts (with respect to 920 cm^{-1}) vs pressure.

Fig. 14. Schematic representation of the Raman-induced Kerr effect spectroscopy experiment. SHG - second harmonic generator; Harm. Sep. - harmonic separator; OMA - optical multichannel analyzer; Sample - benzene.

Fig. 15. Raman-induced Kerr effect spectra (RIKES) of an ambient and two shock-compressed liquid benzene samples. The shock pressure was 1.17 GPa and the 557.03 nm and 556.22 nm Kr calibration lines are shown. All spectra are obtained at the same power levels.

Fig. 16. Vibrational energy levels, some overtones and combinations and infrared spectra: CH_2Cl_2, CH_2Br_2 and CH_2I_2. The vibrational relaxation times, τ_1, shown with the infrared absorption spectra are the measured energy decay times of the CH stretching modes.

Fig. 17. Pressure dependent vibrational relaxation time experiment.

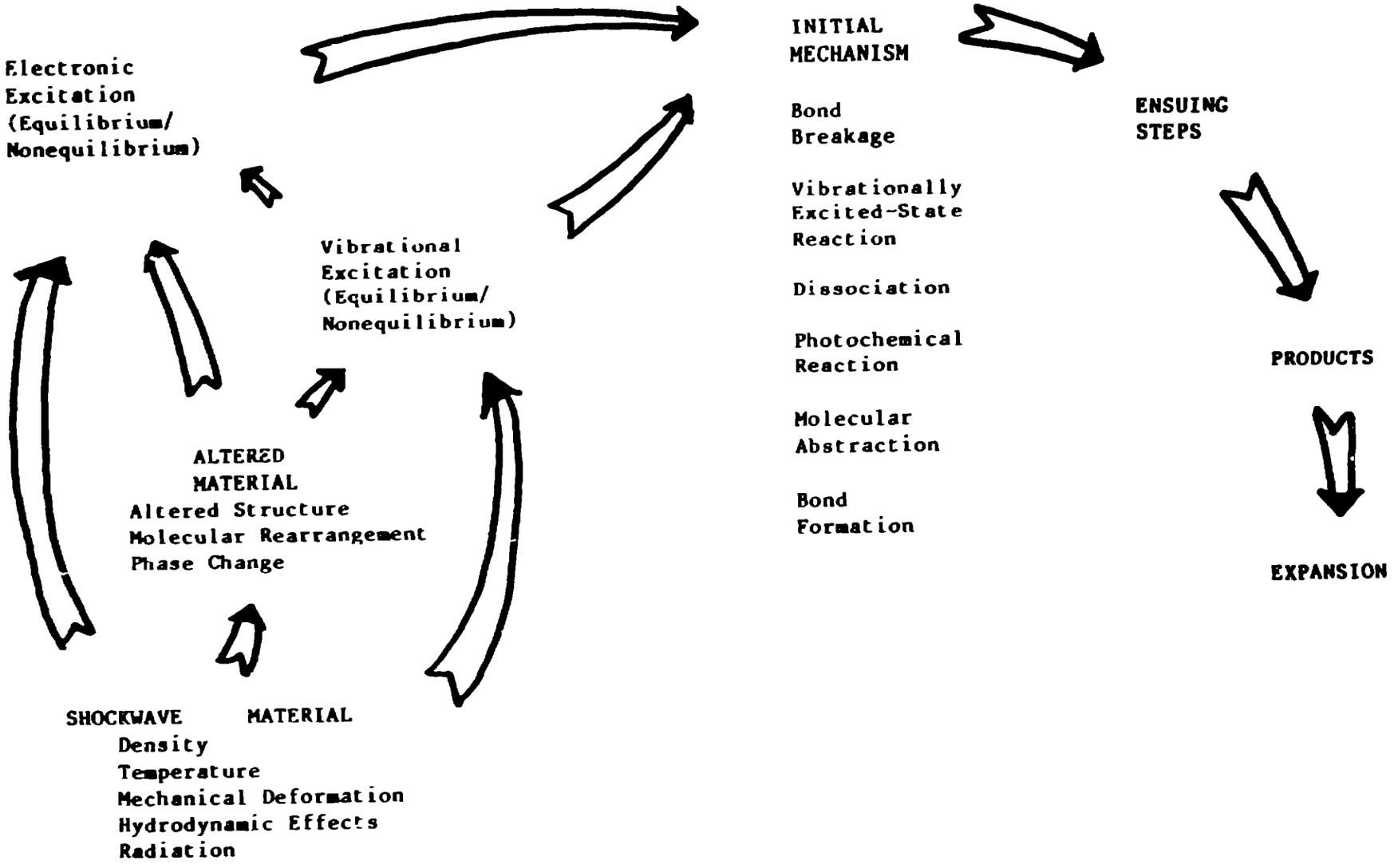
Electronic
Excitation
(Equilibrium/
Nonequilibrium)
Vibrational
Excitation
(Equilibrium/
Nonequilibrium)
ALTERED
MATERIAL
Altered Structure
Molecular Rearrangement
Phase Change
SHOCKWAVE
MATERIAL
Density
Temperature
Mechanical Deformation
Hydrodynamic Effects
Radiation
INITIAL
MECHANISM
Bond
Breakage
Vibrationally
Excited-State
Reaction
Dissociation
Photochemical
Reaction
Molecular
Abstraction
Bond
Formation
ENSUING
STEPS
PRODUCTS
EXPANSION

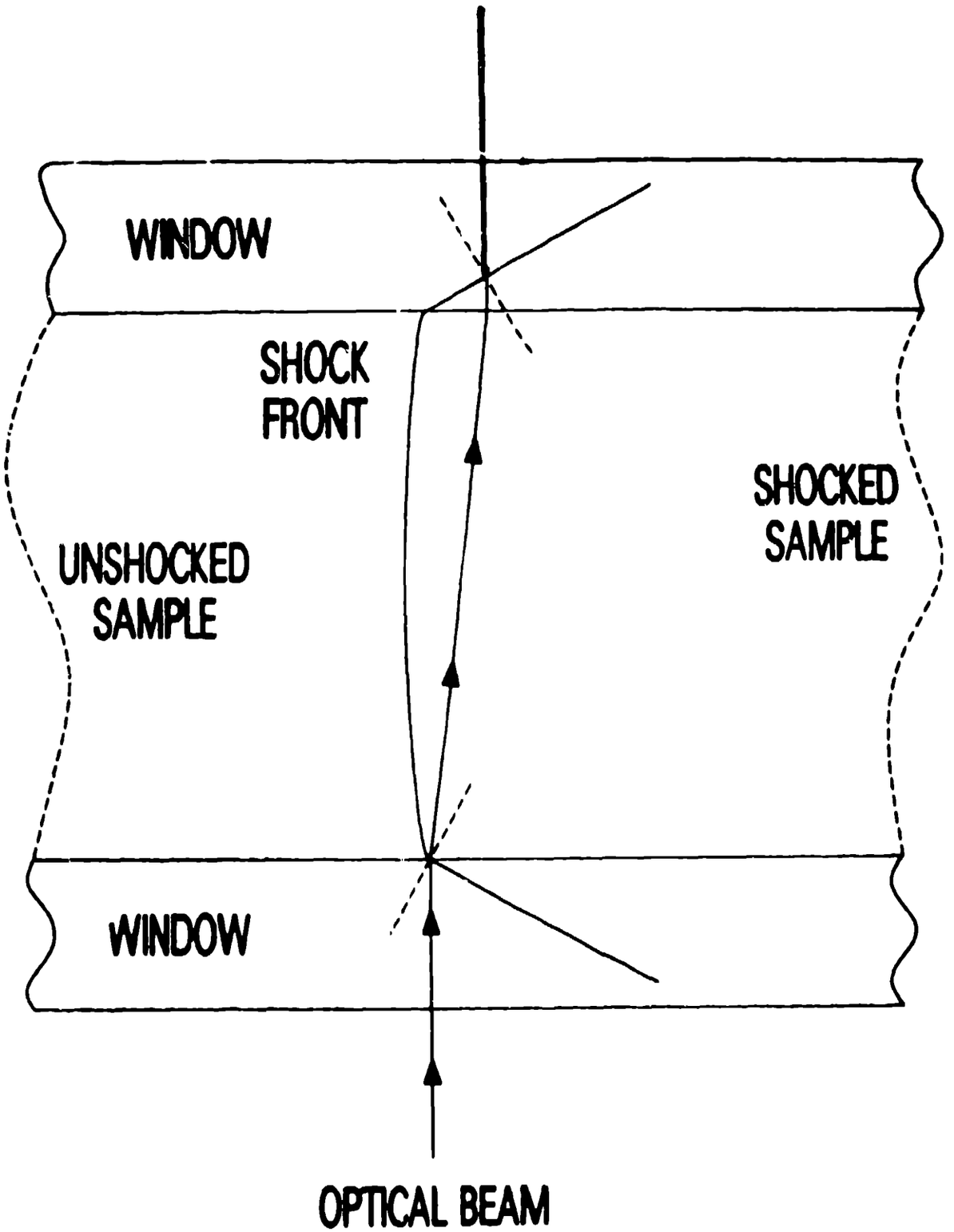
WINDOW
SHOCK
FRONT
SHOCKED
SAMPLE
UNSHOCKED
SAMPLE
WINDOW
OPTICAL BEAM

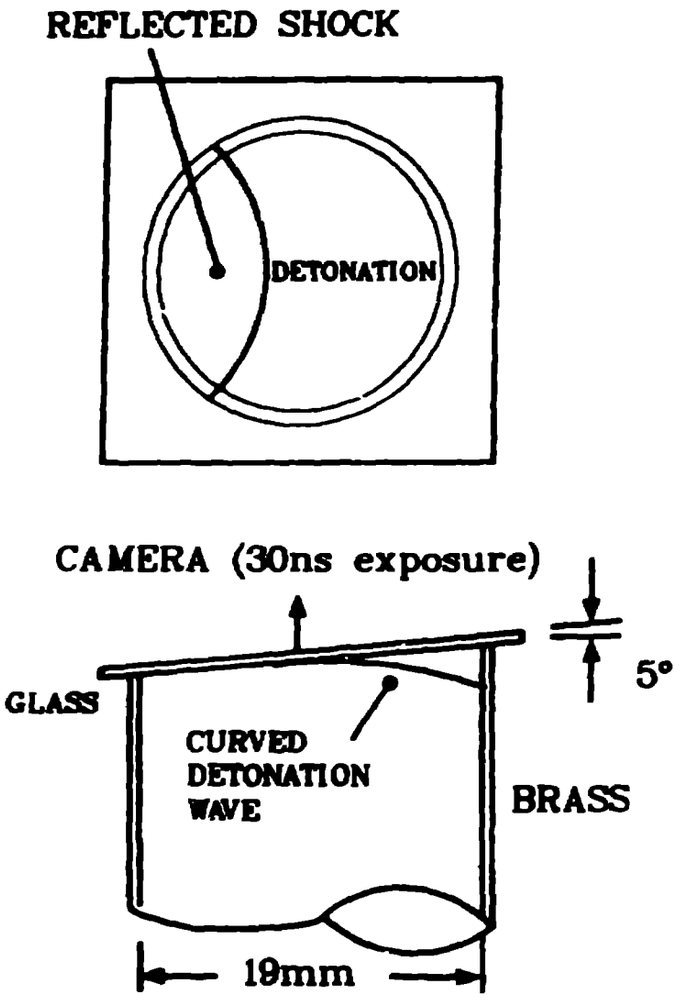

FROM DAVIS

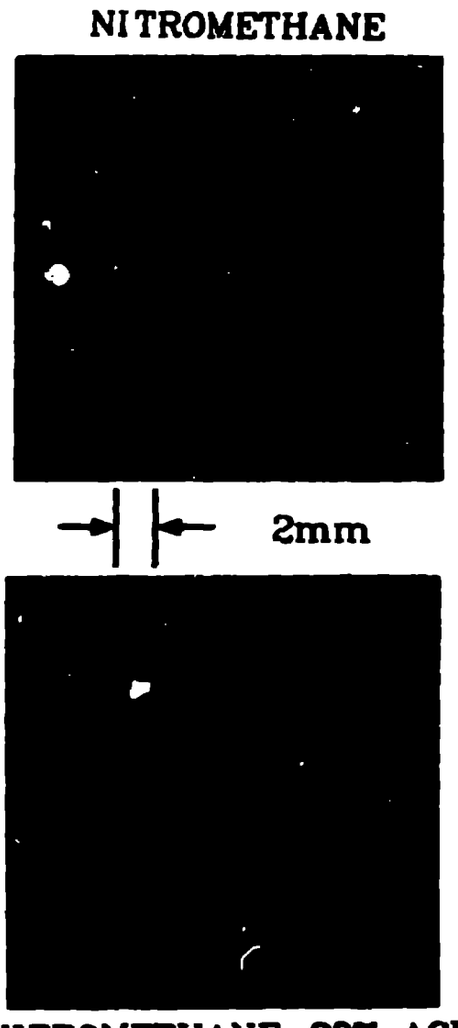

80% NITROMETHANE, 20% ACETONE

HIGHER ORDER RAMAN EXCITATION SPECTROSCOPY
THREE INPUT FREQUENCIES

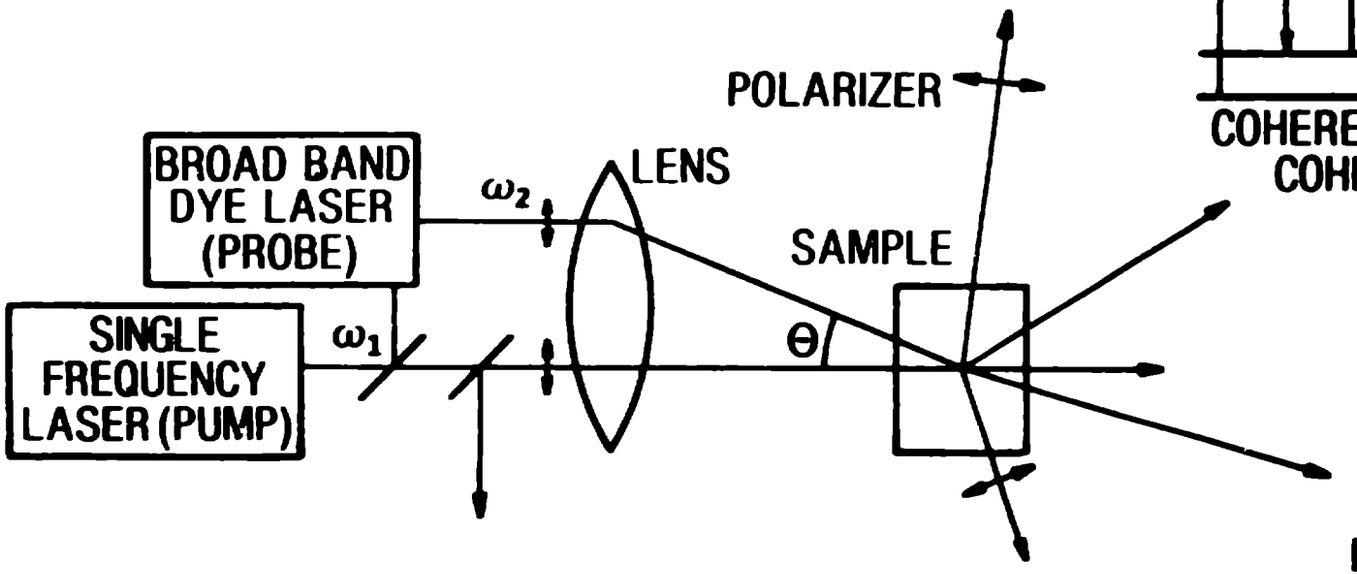

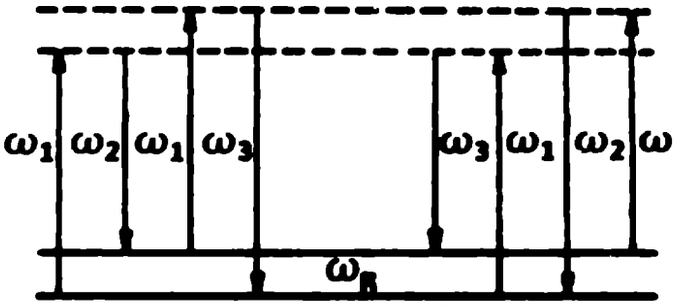

COHERENT ANTI-STOKES RAMAN
COHERENT STOKES RAMAN

STIMULATED RAMAN

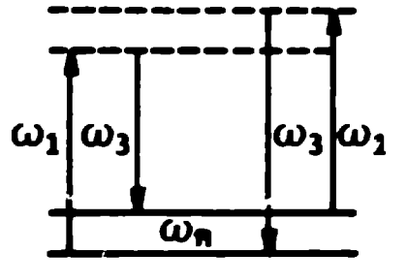

RAMAN INDUCED KERR EFFECT

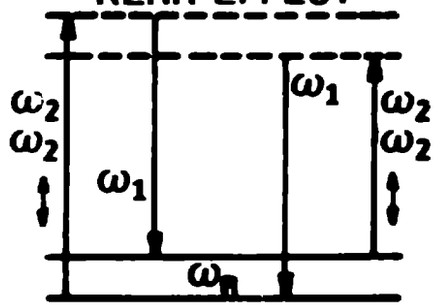

INVERSE RAMAN

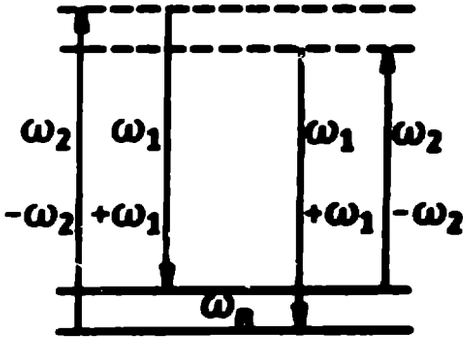

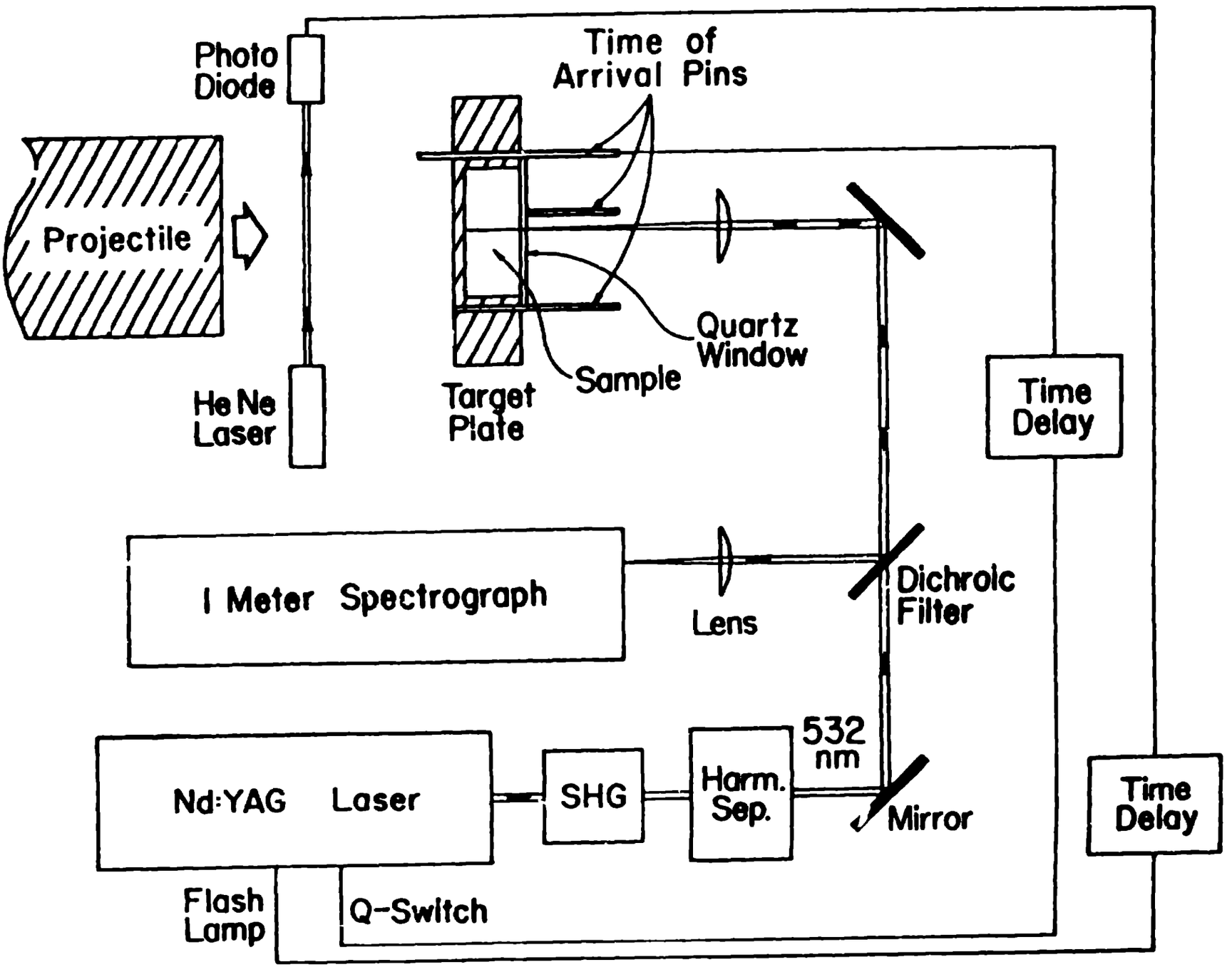
Photo Diode
Time of Arrival Pins
Projectile
Quartz Window
Sample
Target Plate
He Ne Laser
Time Delay
1 Meter Spectrograph
Lens
Dichroic Filter
532 nm
Nd:YAG Laser
SHG
Harm. Sep.
Mirror
Time Delay
Flash Lamp
Q-Switch

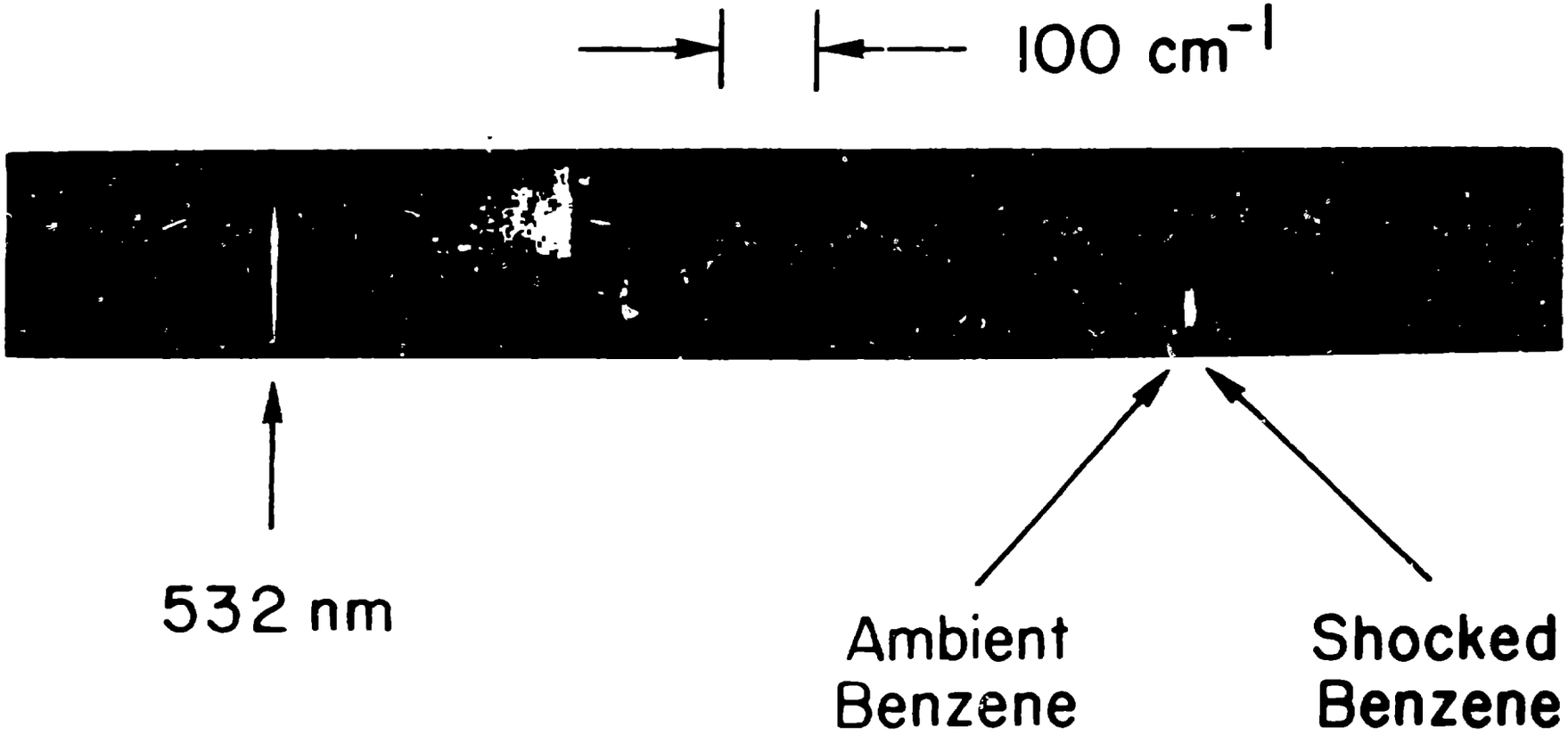
100 cm-1
532 nm
Ambient
Benzene
Shocked
Benzene

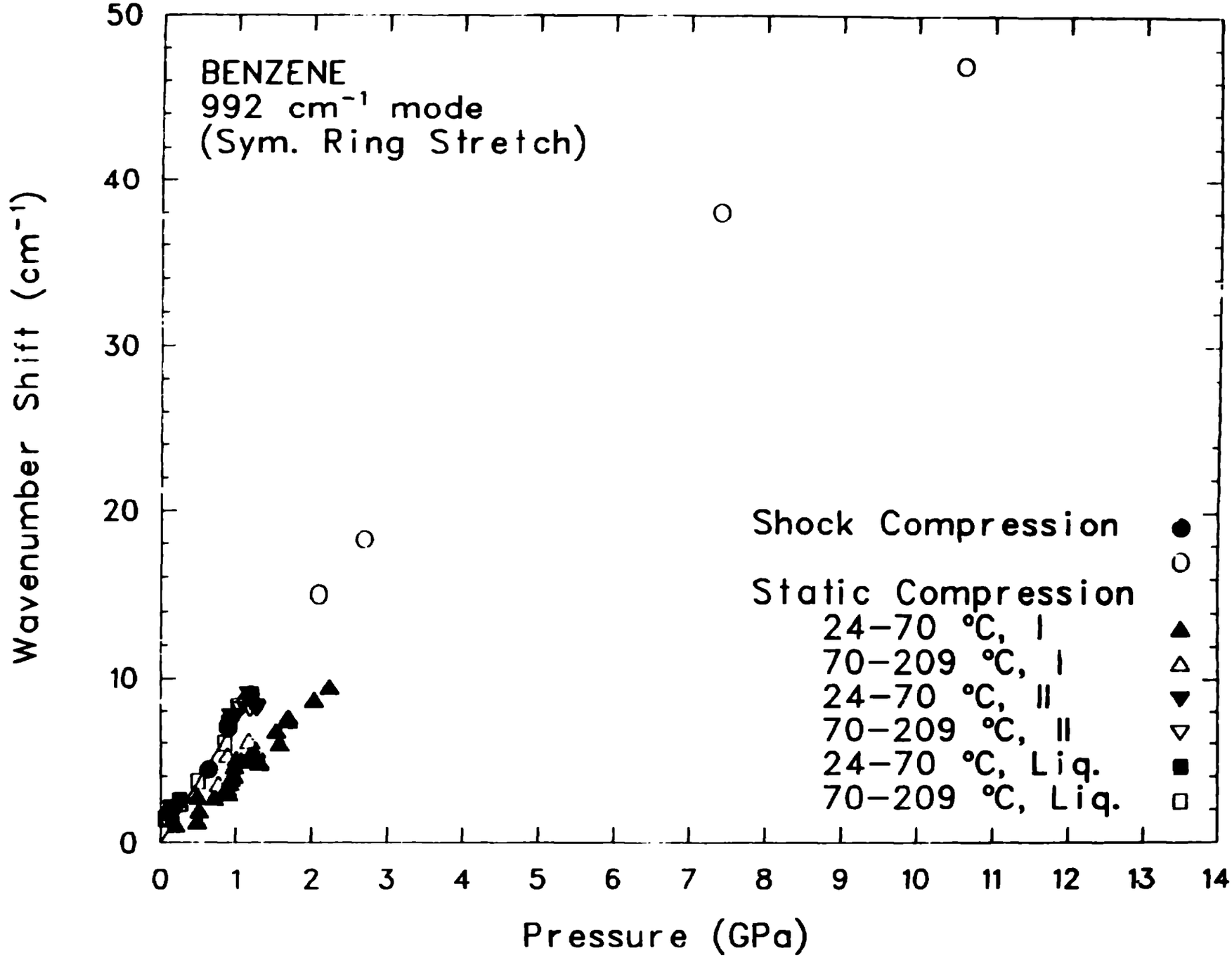
BENZENE
992 cm⁻¹ mode
(Sym. Ring Stretch)
Wavenumber Shift (cm⁻¹)
Pressure (GPa)
0
10
20
30
40
50
0
1
2
3
4
5
6
7
8
9
10
11
12
13
14
Shock Compression
Static Compression
24–70 °C, I
70–209 °C, I
24–70 °C, II
70–209 °C, II
24–70 °C, Liq.
70–209 °C, Liq.

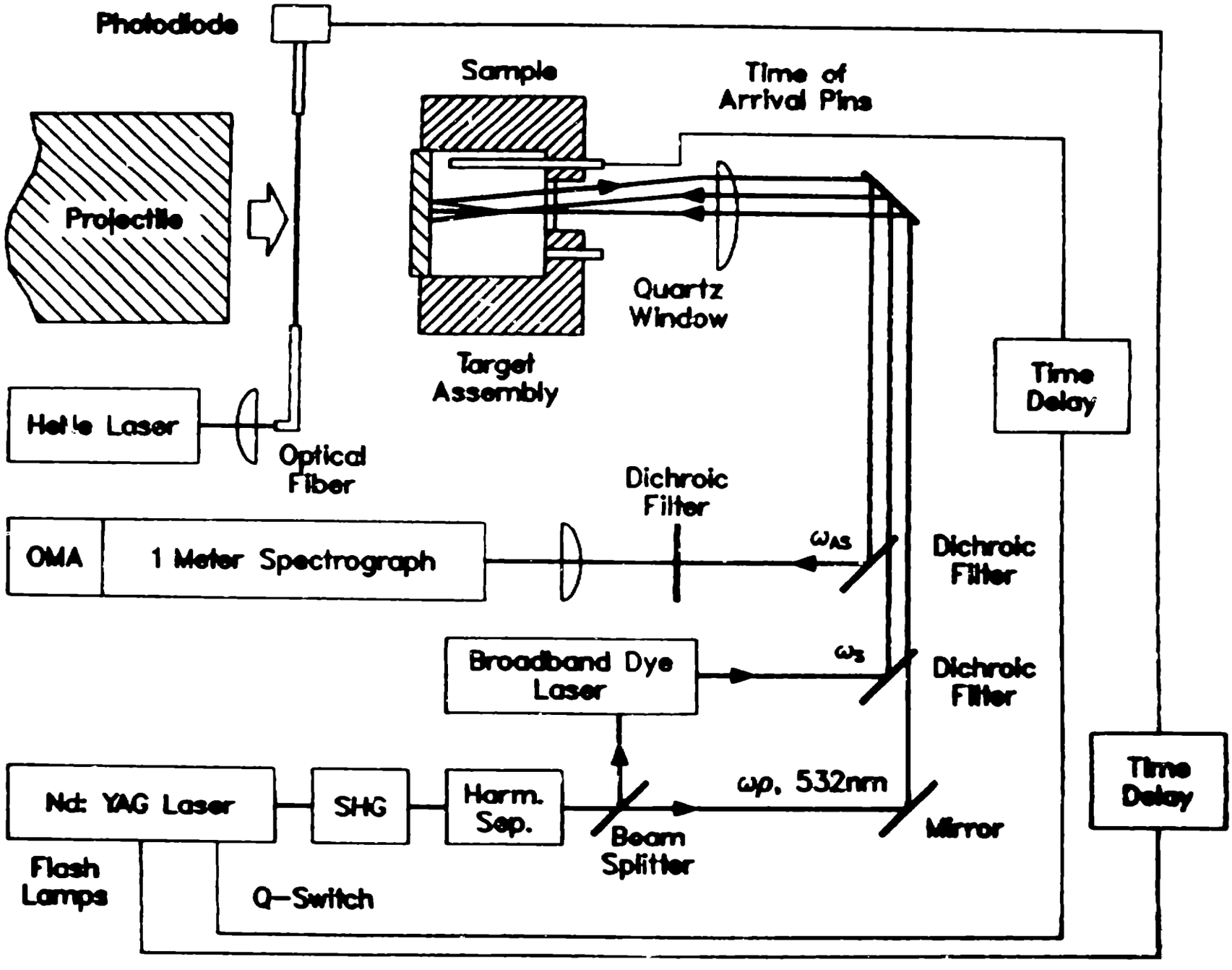
Photodiode
Sample
Time of Arrival Pins
Projectile
Quartz Window
Target Assembly
Time Delay
He-Ne Laser
Optical Fiber
Dichroic Filter
OMA
1 Meter Spectrograph
ω_{AS}
Dichroic Filter
Broadband Dye Laser
ω_S
Dichroic Filter
Nd: YAG Laser
SHG
Harm. Sep.
ωp, 532nm
Time Delay
Beam Splitter
Mirror
Flash Lamps
Q-Switch

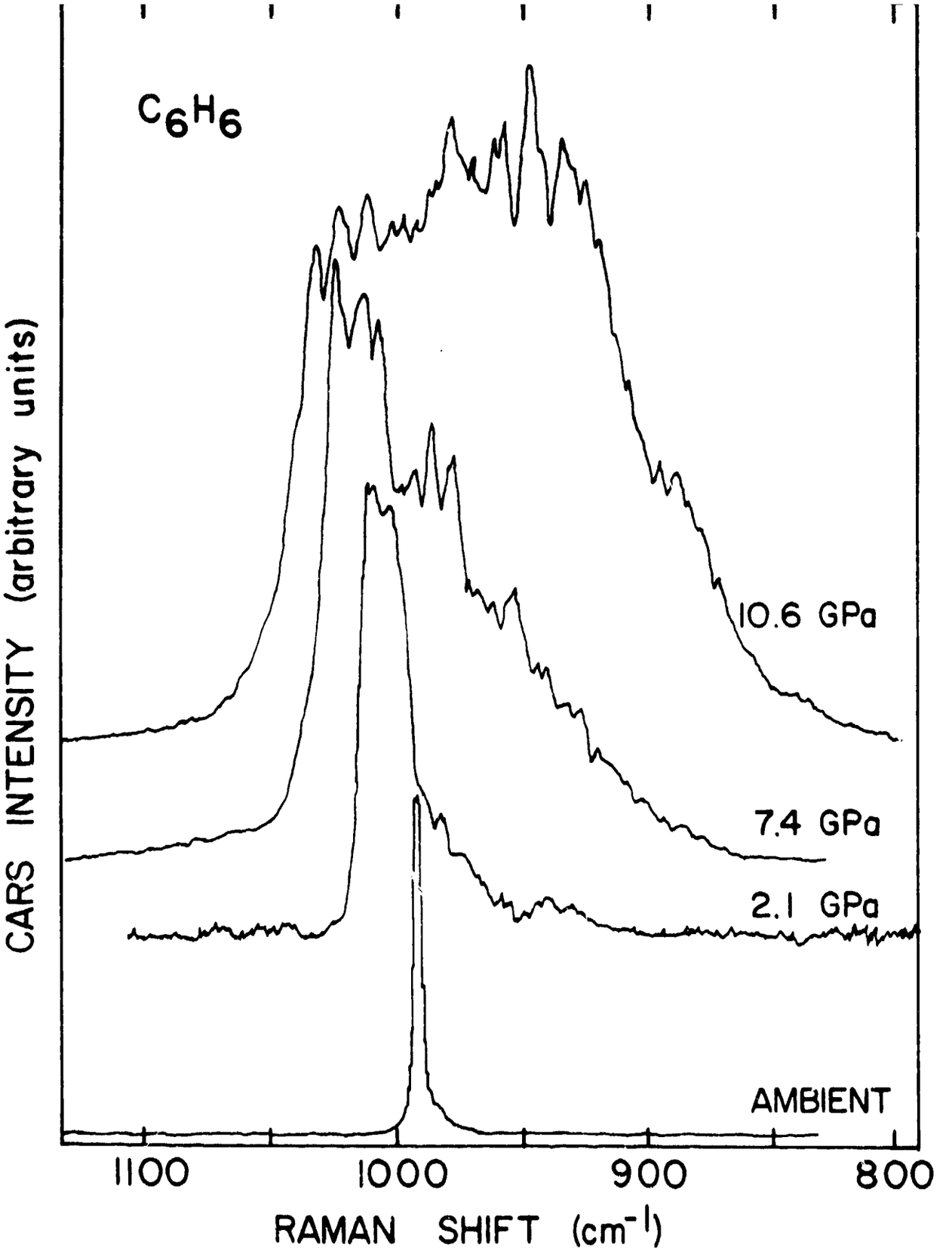
C_6H_6
CARS INTENSITY (arbitrary units)
10.6 GPa
7.4 GPa
2.1 GPa
AMBIENT
1100
1000
900
800
RAMAN SHIFT (cm^{-1})

CHM-VG-8196

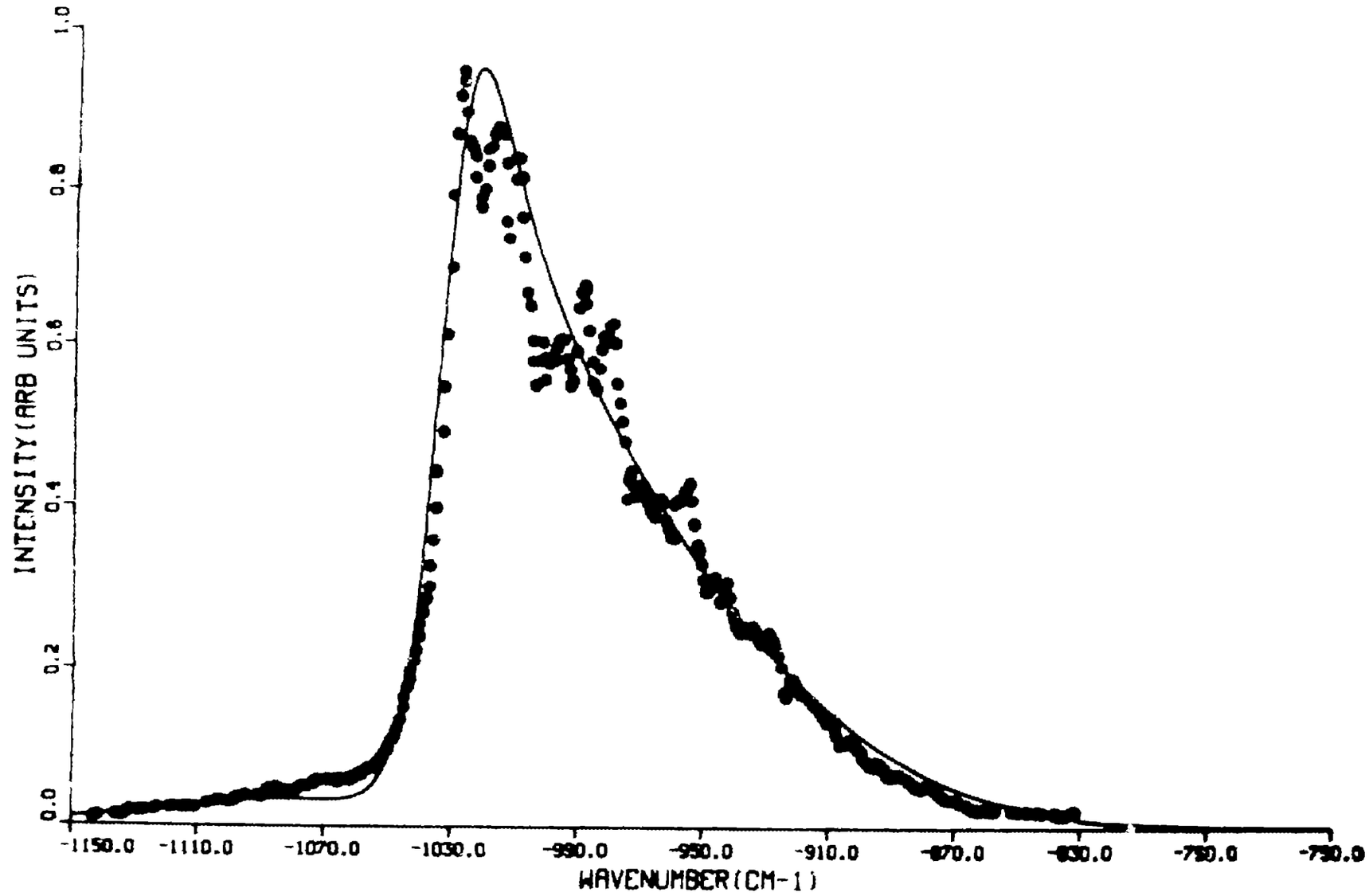
INTENSITY(ARB UNITS)
0.0
0.2
0.4
0.6
0.8
1.0
-1150.0
-1110.0
-1070.0
-1030.0
-990.0
-950.0
-910.0
-870.0
-830.0
-790.0
-750.0
WAVENUMBER(CM-1)

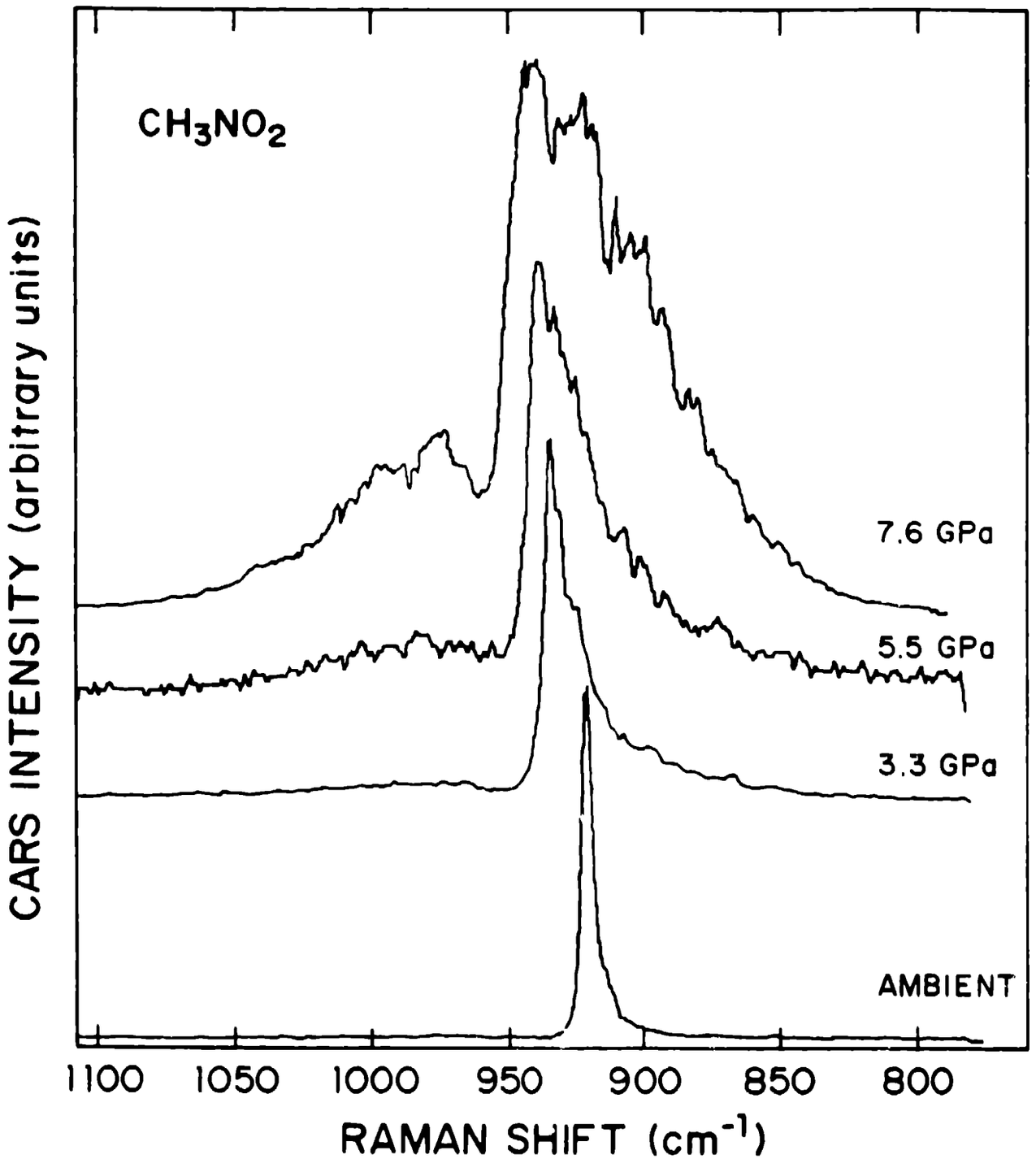
CH_3NO_2
7.6 GPa
5.5 GPa
3.3 GPa
AMBIENT
CARS INTENSITY (arbitrary units)
1100
1050
1000
950
900
850
800
RAMAN SHIFT (cm^{-1})

CHM-VG-8159

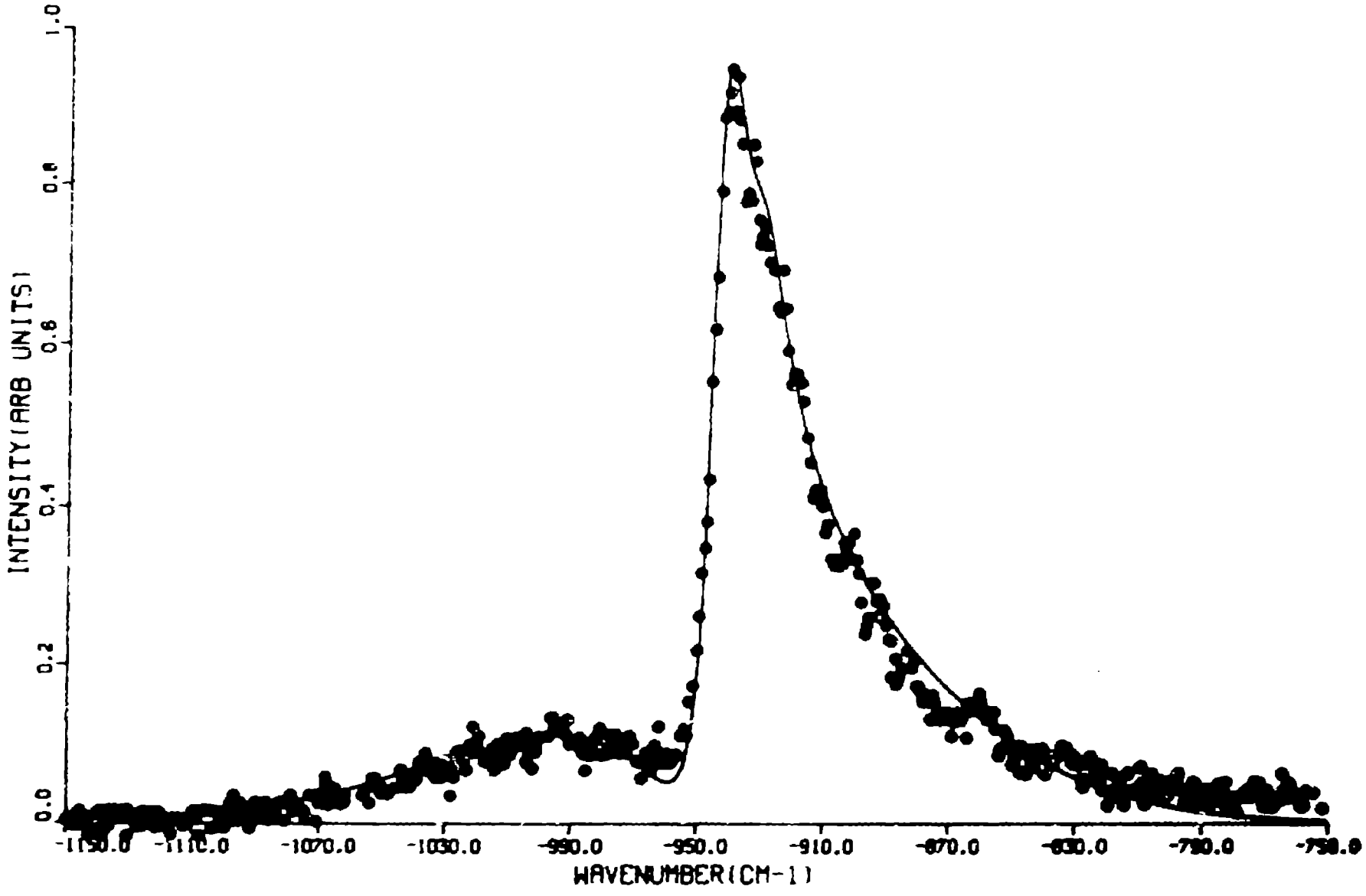
INTENSITY(ARB UNITS)
0.0
0.2
0.4
0.6
0.8
1.0
-1150.0
-1110.0
-1070.0
-1030.0
-990.0
-950.0
-910.0
-870.0
-830.0
-790.0
-750.0
WAVENUMBER(CM-1)

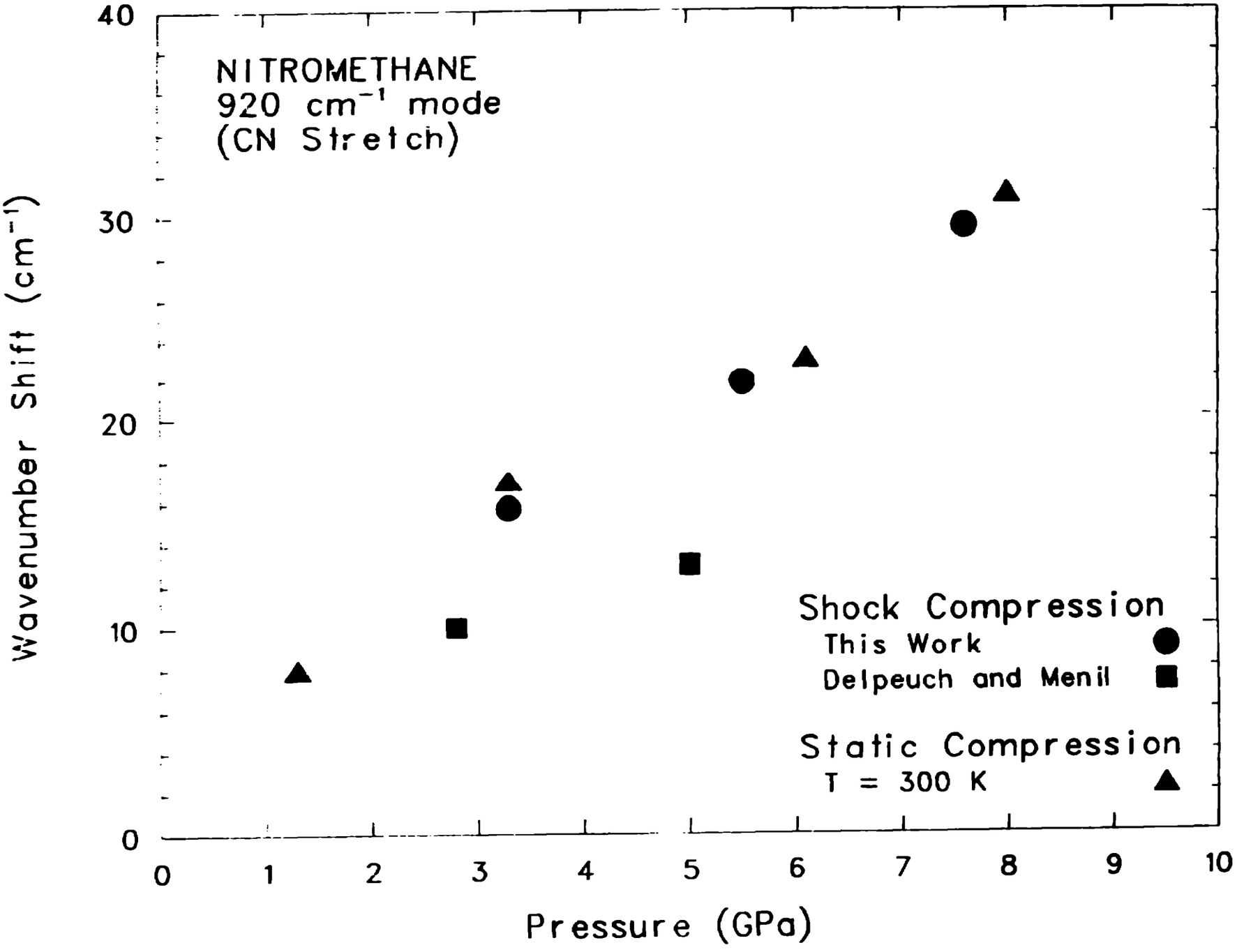
NITROMETHANE
920 cm⁻¹ mode
(CN Stretch)
Wavenumber Shift (cm⁻¹)
Pressure (GPa)
0
10
20
30
40
0
1
2
3
4
5
6
7
8
9
10
Shock Compression
This Work
Delpeuch and Menil
Static Compression
T = 300 K

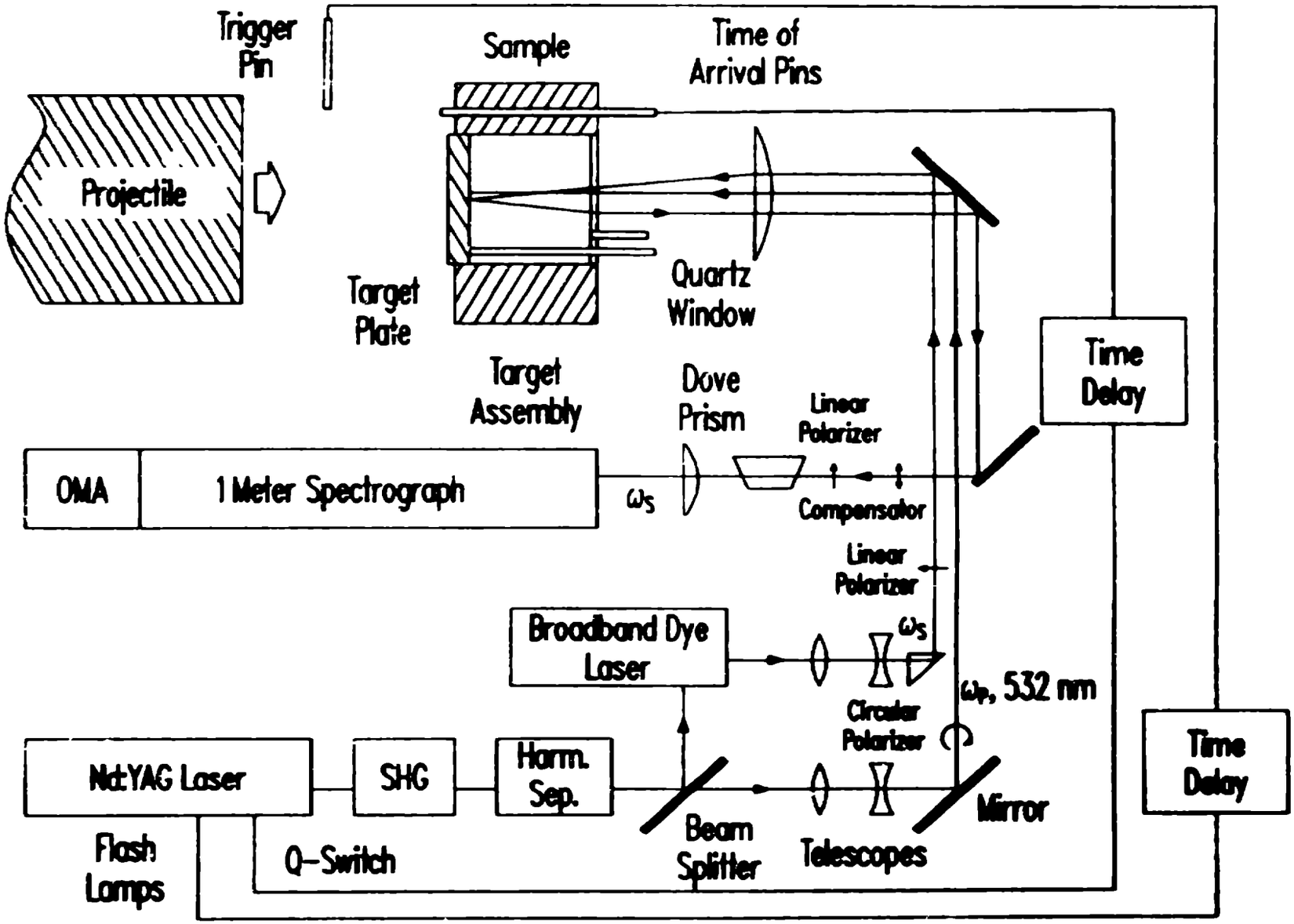
Trigger Pin
Sample
Time of Arrival Pins
Projectile
Target Plate
Quartz Window
Target Assembly
Dove Prism
Linear Polarizer
Time Delay
OMA
1 Meter Spectrograph
ω_S
Compensator
Linear Polarizer
Broadband Dye Laser
ω_S
ω_P, 532 nm
Circular Polarizer
Nd:YAG Laser
SHG
Harm. Sep.
Beam Splitter
Mirror
Telescopes
Time Delay
Flash Lamps
Q-Switch

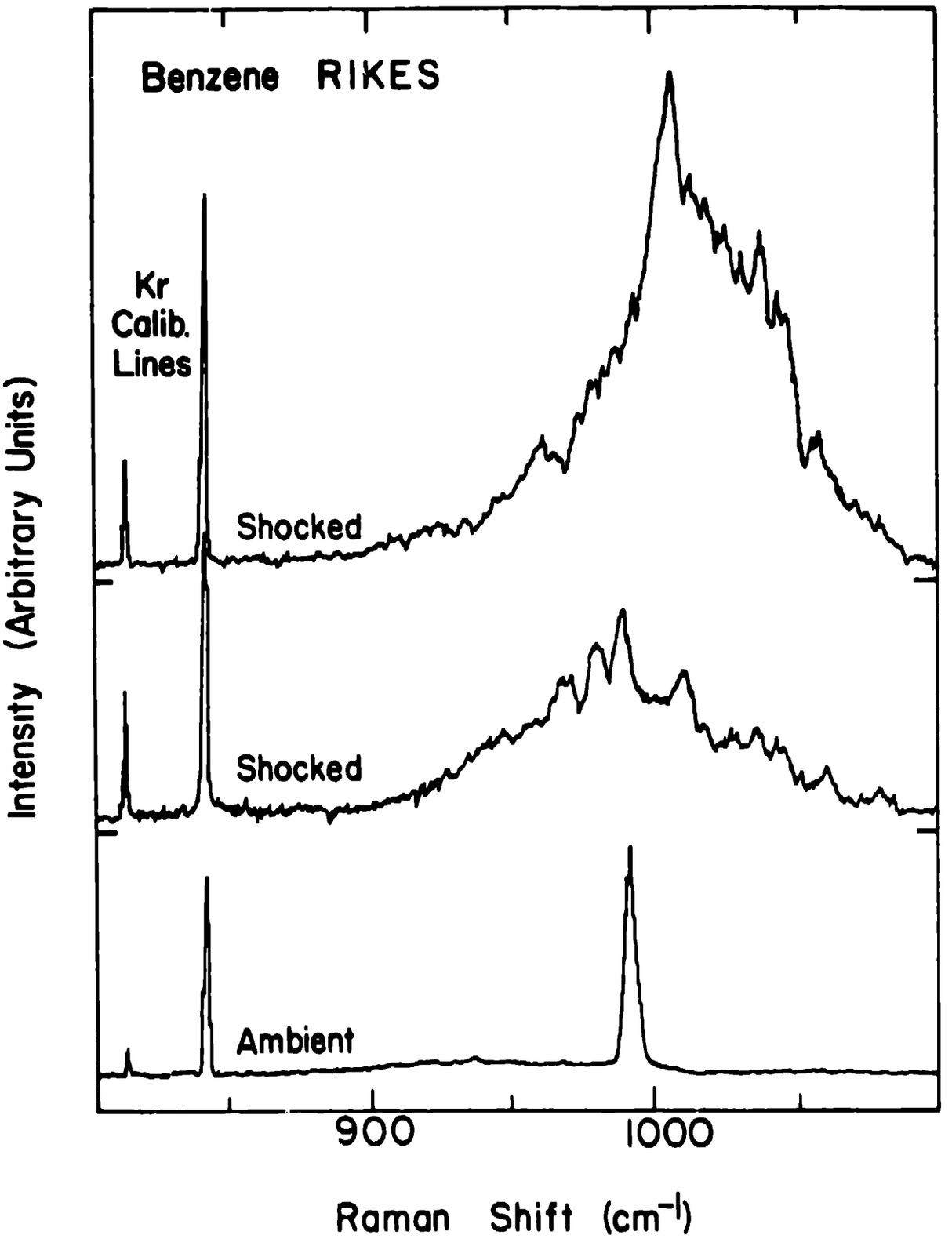
Benzene RIKES
Kr
Calib.
Lines
Shocked
Shocked
Ambient
Intensity (Arbitrary Units)
900
1000
Raman Shift (cm⁻¹)

VIBRATIONAL MODES AND INFRARED SPECTRA
(from Graener and Laubereau)

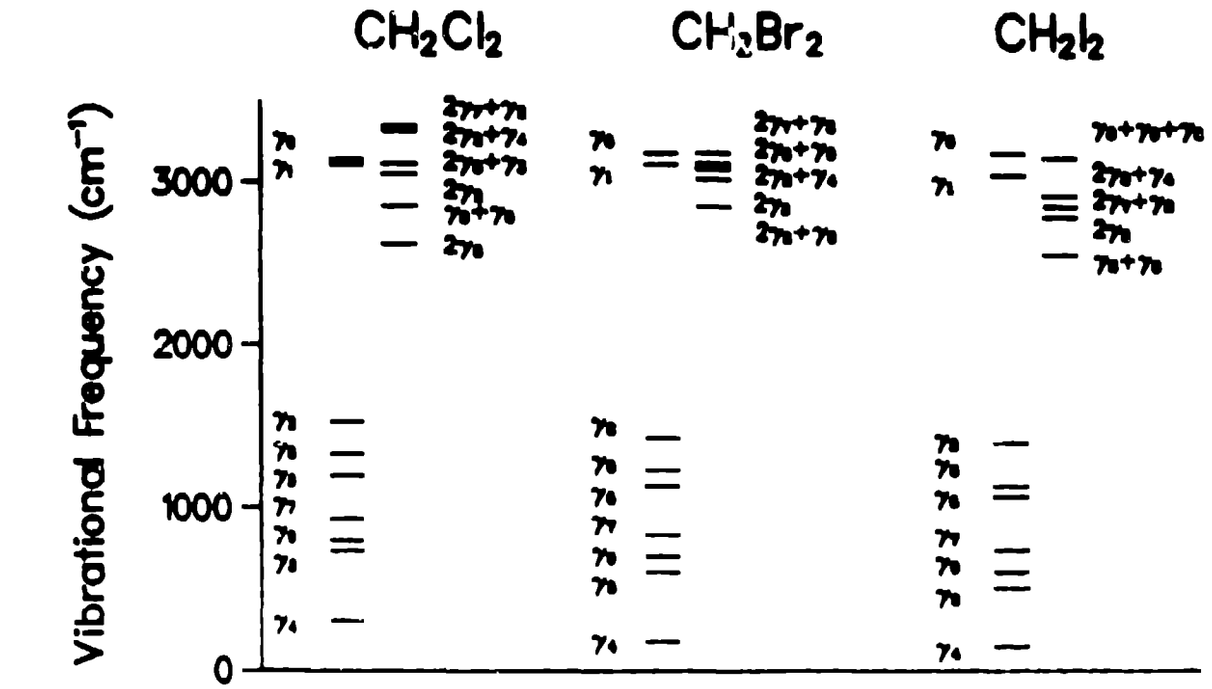

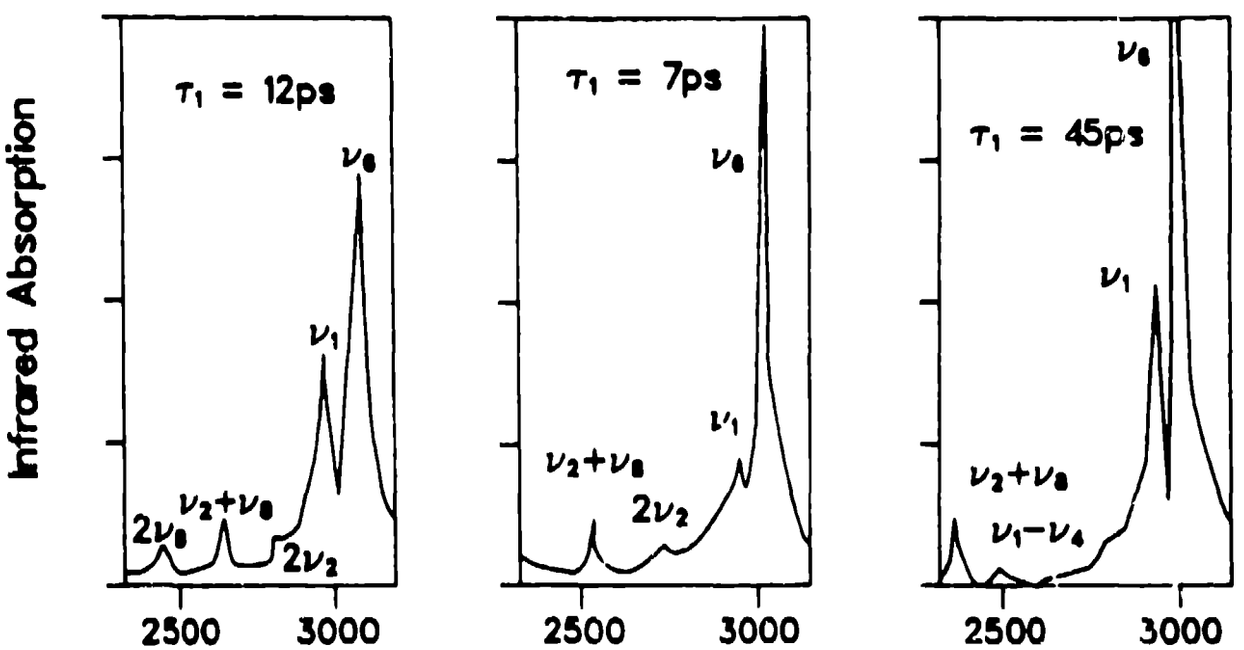

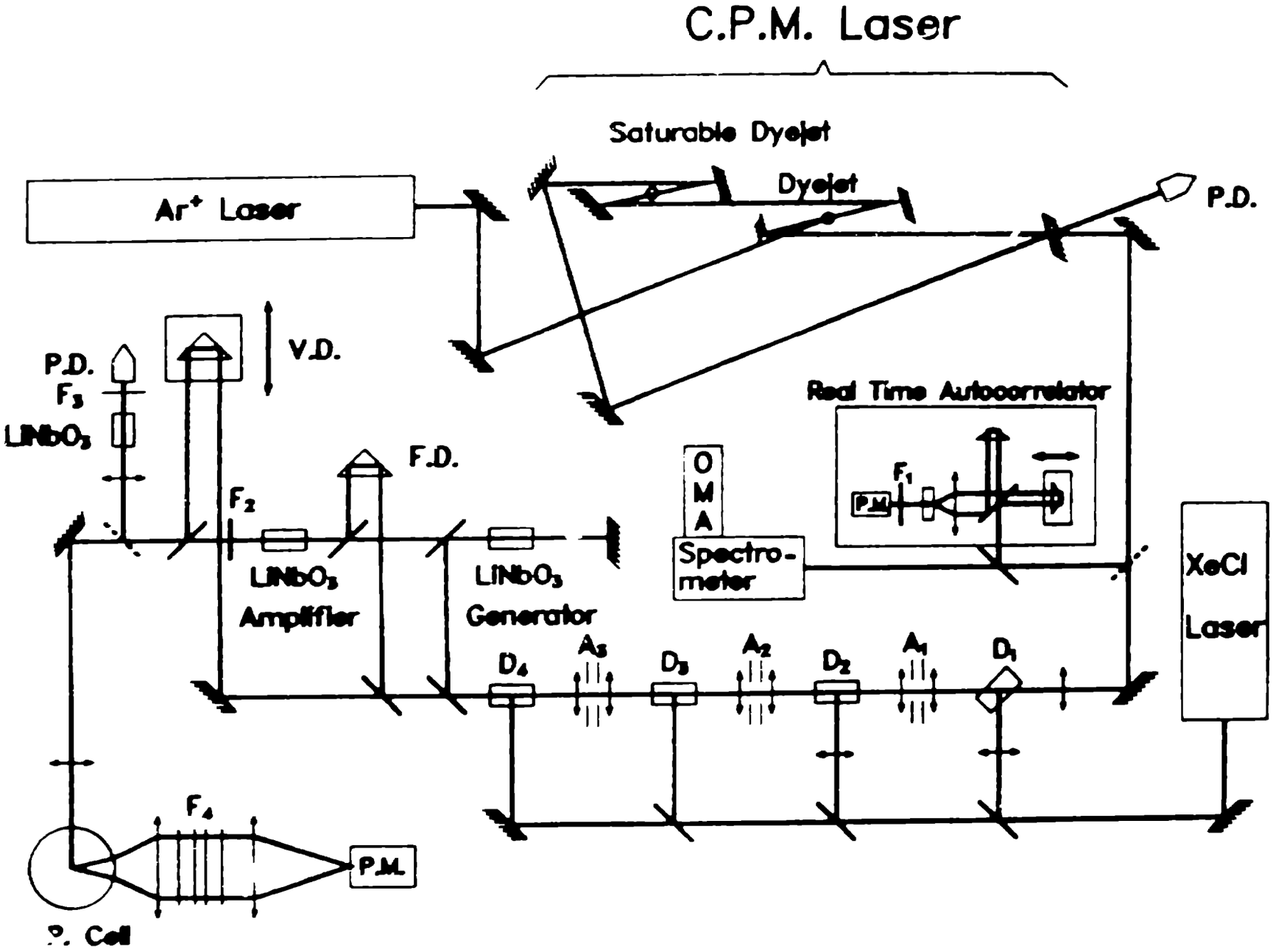
C.P.M. Laser
Saturable Dyejet
Dyejet
Ar+ Laser
P.D.
V.D.
P.D.
F3
LINbO3
F.D.
F2
Real Time Autocorrelator
F1
P.M.
OMA
Spectro-
meter
LINbO3
Amplifier
LINbO3
Generator
XeCl
Laser
D4
A3
D3
A2
D2
A1
D1
F4
P.M.
Cell